Available online at www.sciencedirect.com

ScienceDirect

Geochimica et Cosmochimica Acta 140 (2014) 142–159

Geochimica et Cosmochimica Acta

www.elsevier.com/locate/gca

Assessment of the clumped isotope composition of fossil bone carbonate as a recorder of subsurface temperatures

Marina B. Suarez *, Benjamin H. Passey

Johns Hopkins University, Department of Earth and Planetary Sciences, 3400 N. Charles St., Baltimore, MD 21218, USA

Received 13 August 2013; accepted in revised form 19 May 2014; Available online 29 May 2014

Abstract

Bone is susceptible to early diagenesis, and its carbon and oxygen isotopic compositions have been suggested to reflect conditions in the soil environment and shallow subsurface during fossilization. This implies open-system recrystallization involving mass exchange of carbon and oxygen among bioapatite, soil water, and DIC. Such recrystallization would also redistribute isotopic clumping (including ^{13}C–^{18}O bonds), leading to the possibility that the carbonate clumped isotope compositions of fossil bone record ground temperature during early diagenesis. We assess this possibility by studying Quaternary mammalian fossil bone from subtropical to polar latitudes: if recrystallization is early and pervasive, clumped isotope derived temperatures, $T(\Delta_{47})$, should closely mirror latitudinal gradients in ground temperature. Excluding results from a mummified specimen yielding $T(\Delta_{47}) = 38$ °C (that is, indistinguishable from mammalian body temperature), we find that $T(\Delta_{47})$ values are intermediate between mammalian body temperature and ground temperature, suggesting partial recrystallization of bone carbonate. XRD analyses show that the nature and extent of diagenesis varies among the samples and does not relate in a straightforward manner to $T(\Delta_{47})$. No clear correlation exists between $T(\Delta_{47})$ and mean annual temperature or mean warm season temperature. Furthermore, bone tends to retain the ^{18}O-enriched signature of body water, suggesting incomplete oxygen isotope exchange with meteoric waters.

Incomplete carbon and oxygen isotope exchange between bone carbonate and soil waters is also indicated for a set of late Miocene bone–enamel pairs from a sequence of stacked paleosols in northern China. Analysis of bone as old as Early Cretaceous shows that bone carbonate is susceptible to later diagenesis at elevated burial temperatures, although $T(\Delta_{47})$ does not closely conform to maximum burial temperature, again suggesting partial recrystallization, or recrystallization during different stages of the burial and exhumation circuit. These results show that carbon, oxygen, and 'clumped' isotopes in fossil bone are capable of recording aspects of early diagenesis and the subsequent burial and exhumation history, but that distinguishing among different effects is challenging. However, clumped isotopes in bone can provide useful directional constraints on past temperatures. For example, $T(\Delta_{47})$ values higher than body temperature necessarily place lower limits on maximum burial temperatures, and those lower than body temperature place upper limits on minimum fossilization temperatures.

1. INTRODUCTION

Geochemical utilization of fossil vertebrates has been a target of paleontological and archaeological research for at least 30 years (Kolodny et al., 1983; DeNiro, 1987; Lee-Thorp and Van der Merwe, 1987; Kohn, 1996; Barrick et al., 1999; Amiot et al., 2010, and many others). The consensus of most researchers is that the carbonate

* Corresponding author. Present address: University of Texas at San Antonio, Department of Geological Sciences, One UTSA Blvd., San Antonio, TX 78249, USA. Tel.: +1 210 458 8596.
E-mail address: marina.suarez@utsa.edu (M.B. Suarez).

http://dx.doi.org/10.1016/j.gca.2014.05.026
0016-7037/

component of enamel bioapatite generally records primary (biogenic) $\delta^{13}C$ and $\delta^{18}O$ compositions, whereas the carbonate component of bioapatite in bone and dentine commonly shows evidence of alteration, and may reflect the diagenetic environment of fossilization (Schoeninger and DeNiro, 1982; Kohn and Law, 2006; Tütken et al., 2008). This difference is primarily related to the greater porosity, higher organic content, and smaller bioapatite crystallites in bone and dentine compared to tooth enamel (Ayliffe et al., 1994; Kohn et al., 1999; Kohn and Cerling, 2002; Trueman and Tuross, 2002; Zazzo et al., 2004). In this paper, we consider 'the carbonate component' of bone, or 'bone carbonate', to include any phosphoric acid-extractable carbonate that remains in bone, dentine, or cementum following standard pretreatment protocols (see Section 3) designed to remove nonbioapatite carbonate phases such as calcite.

Kohn and Law (2006) examined the paleoenvironmental utility of carbon and oxygen isotopes in bone carbonate. Their study of bone preserved in late Paleogene and Neogene fluvial sediments and associated paleosols suggests that a diagenetic composition is incorporated into bone over ~20–50 ka timescales, similar to the thousands or tens of thousands of year timescales for fossilization inferred from the study of late Quaternary bone (e.g., Tuross et al., 1989; Trueman and Tuross, 2002). They suggest that the carbon and oxygen isotopic compositions of bone carbonate are similar to the isotopic compositions of soil carbonate in the overlying paleosol. Once recrystallized, bone is presumably more resistant to further isotopic alteration, and therefore is capable of preserving the isotopic signature of the diagenetic environment over geological timescales. A number of recent studies, however, indicate further diagenetic alteration may occur, particularly in the exchange or addition of REEs but also in compositional changes (Piga et al., 2009; Kocsis et al., 2010; Tütken et al., 2011). If bone carbonate does preserve its early diagenetic isotope composition, it could be used in an analogous manner to isotopes in soil carbonate, that is, as recorders of the $\delta^{13}C$ of prevailing vegetation, and of the $\delta^{18}O$ of soil water, itself a function of precipitation $\delta^{18}O$ and soil water evaporation processes (Kohn and Zanazzi, 2008). Such a tool would be especially advantageous in strata with sparse or no soil carbonates, but abundant vertebrate fossil material. This method has already been applied to the reconstruction of past environments, including climate change in North America during the Eocene–Oligocene transition (Zanazzi et al., 2007), and paleoelevation reconstruction of the Tibetan Plateau (Wang et al., 2013).

The advent of the carbonate clumped isotope paleothermometer (Ghosh et al., 2006; Schauble et al., 2006) now allows temperature information to be retrieved from materials as diverse as corals (Thiagarajan et al., 2011), foraminifera (Tripati et al., 2010), soil carbonates (Quade et al., 2013) and bioapatite (Eagle et al., 2010, 2011). Briefly, the clumped isotope paleothermometer is based on the thermodynamic tendency for ^{13}C and ^{18}O to "clump" together to form multiply substituted isotopologues of carbonate (Schauble et al., 2006). These clumps increase in abundance with decreasing temperature, and laboratory-based and empirical equations have been developed relating the parameter Δ_{47} (a measure of isotopic clumping in CO_2 generated from carbonate by phosphoric acid digestion) to mineral growth temperature (Ghosh et al., 2006; Eiler, 2007). Eagle et al. (2010) conducted an initial investigation into isotopic clumping in recent (pristine) bioapatite of mammals, fish, and reptiles, and demonstrated that the Δ_{47}–T relationship is indistinguishable from that of laboratory-precipitated calcite and biogenic calcite and aragonite. Furthermore, the clumped isotope derived temperature, $T(\Delta_{47})$, determined from tooth enamel was shown to accurately reflect animal body temperature, and the technique was subsequently used to reconstruct body temperatures of dinosaurs (Eagle et al., 2011). During these investigations it was shown that dentine and bone generally do not preserve original body temperature and rather reflect a diagenetic value, whereas enamel is most likely to retain bond ordering reflective of original body temperature.

The goal of this study is to evaluate the potential utility of this diagenetic $T(\Delta_{47})$ signal in dentine and bone by examining a suite of Quaternary and pre-Quaternary fossils. We hypothesize that if bond ordering of carbonate in bone is reset in the early diagenetic fossilization environment, clumped isotope derived temperatures of Quaternary mammal bone will show a latitudinal gradient similar to or steeper than the modern latitudinal temperature gradient of mean annual temperature (MAT) or mean warm season temperature (MWST, mean temperature of the three warmest months of the year) (Fig. 1). If bond ordering of bone carbonate is only partially reset during fossilization, temperatures will be intermediate between mammal body temperature (~38 °C) and MAT or MWST. In addition to our study of Quaternary bone, we examined older bone to evaluate the behavior of the carbonate component of bone during later burial and exhumation.

2. SAMPLE MATERIAL

2.1. Quaternary bone

We examined bone from polar (Alaska), temperate (South Dakota, Kansas) and subtropical latitudes (Florida, South Africa). Fragments of mammoth and bison bone were cut from identified specimens housed in the Museum of the North at the University of Alaska at Fairbanks. All samples come from within approximately 1° of latitude from each other (65.5–66.2°N; see Table 1 for coordinates). Included in this set of samples was a rib (UAMES-4588) from a mummified bison (*Bison priscus*) called 'Blue Babe' dated at about 36,000 years (Guthrie, 1988, 1990) and recovered from remobilized loess (locally termed "muck") approximately 26 km northeast of Fairbanks, Alaska in 1979. The other Alaskan fossils were collected from loess deposits or river gravel deposits. Sample UAMES-4517 is a mammoth tibia fragment recovered in 1961 near Elephant Point on the Seward Peninsula. Its exact depositional context is unknown, but the majority of fossils found in this area are found eroding out of loess deposits. Two mammoth bone fragments were sampled from material collected between 1984 and 1987 along the banks of the Koyukuk

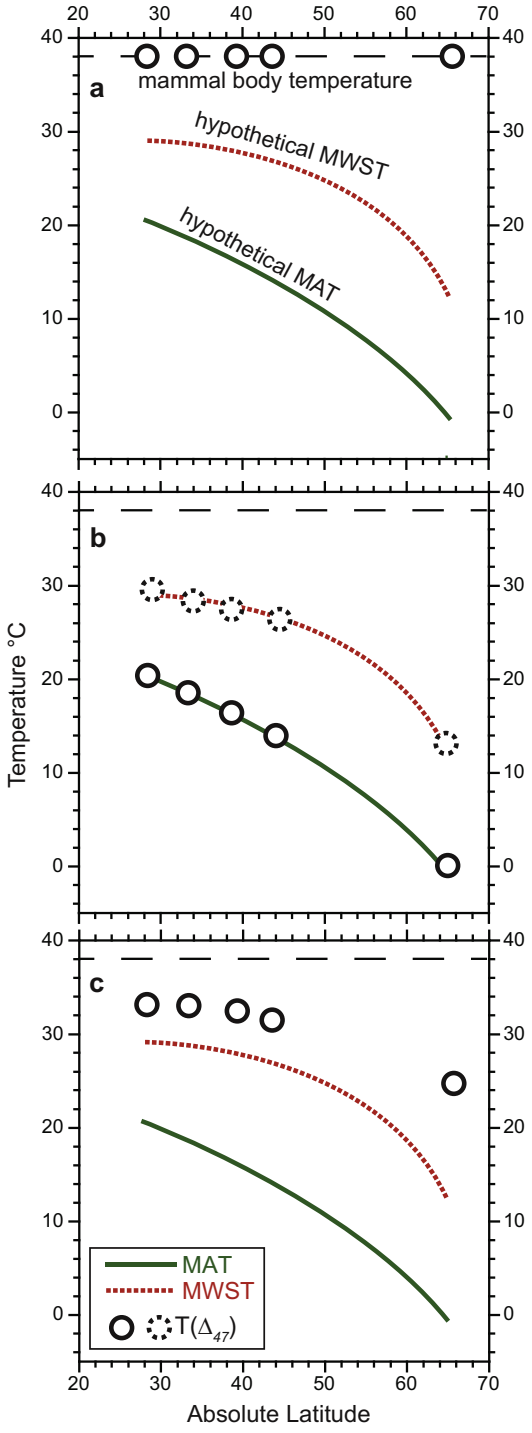

Fig. 1. Hypothetical initial conditions and diagenetic scenarios for the clumping of carbon and oxygen in bioapatites during fossilization. (a) Initial conditions: mammal body temperature of approximately 38 °C is reflected in $T(\Delta_{47})$ of bone carbonate. (b) Diagenetic Scenario 1: bone carbonate $T(\Delta_{47})$ reflects mean annual temperature (solid circles and solid line) or mean warm season temperature (dashed circles and dashed line) suggesting complete redistribution of ^{13}C–^{18}O bonds. (c) Diagenetic Scenario 2: bone carbonate $T(\Delta_{47})$ reflects temperatures between mammal body temperature and MAT or MWST suggesting partial redistribution of ^{13}C–^{18}O bonds.

River in the Kateel River USGS Quadrangle. These specimens do not have exact depositional information associated with them, but they likely were eroded from river bluffs and deposited in river gravels.

Samples from temperate latitudes come from Kansas and South Dakota. We sampled bone and dentine from the Mammoth Site, Hot Springs, South Dakota, a sinkhole accumulation preserving dozens of skeletons of mammoths and other species. The sinkhole was likely filled with water, and the sediment surrounding the skeletons grades from gravels near the base associated with the erosion of the breccia pipe collapse, to fine, laminated silts and muds, to bioturbated muds as the sinkhole filled with sediment (Laury, 1980). The site is dated between 21,000 and 26,000 years old (Laury, 1980; Agenbroad, 1989; Agenbroad, 2005). Samples from Kansas (Kansas Museum of Natural History) include bone fragments from the genera *Cervacales* (KMNH 119664), *Sus* (KUVP 88518), and *Mylohylus* (KUVP 97035). The *Sus* and *Mylohylus* bone were recovered from sand and gravel bars near Bonner Springs, Kansas along the Kansas River.

Subtropical samples come from Florida and South Africa. The sample collected from Florida is an unidentified large mammal bone opportunistically collected by Dr. Kenneth Rose during dredging of sediments to improve waterways near Venice, Florida in the 1960s. The sample is thought to be Late Pleistocene in age. Samples from Elandsfontein, South Africa are the only samples from the Southern Hemisphere that were analyzed. Elandsfontein is on the southwest coast of South Africa where numerous collections of mammal bone including early hominin bone and artifacts have been collected in ancient dune deposits. The majority of the fossil remains are found in a horizon that appears to be pedogenically modified quartz sand dune deposits. The horizon is often characterized by ferruginous nodules and white siliceous nodules that may have originally been calcareous (Braun et al., 2013). The age of the Elandsfontein accumulation based on biostratigraphy and preliminary magnetostratigraphy is likely between 0.99 and 0.78 Ma (Braun et al., 2013), though Braun et al. (2013) do not rule the possibility that some skeletal remains are older than this age range.

2.2. Pre-Quaternary bone

Bone and dentine samples from as young as Pliocene and as old as Cretaceous were sampled to assess the effects of burial diagenesis on the clumped isotope composition of bone. Sauropod bone fragments were cut from tibia and femur fragments from the Lower Cretaceous Cedar Mountain Formation. The samples come from the Dalton Wells Quarry, just north of Moab, Utah. The bone assemblage has been interpreted to have been deposited in a debris flow (Eberth et al., 2006) and occurs in poorly-sorted muddy sandstones with floating pebbles and cobbles. Bone was sampled from the late Eocene Birket Qarun Formation in the Fayum Depression, Egypt (sample BQ-2), and the overlying early Oligocene Jebel Qatrani Formation (sample L-30). Both formations are primarily fluvial sediments interfingering with nearshore marine sediments (Bown

Table 1
Stable carbon isotope, oxygen isotope, and clumped isotope data from bone, dentin, and ivory samples along with temperature and water isotopic composition.

Location (lat, long)	Sample name (type)	Depositional environment	Period/epoch	N	$\delta^{13}C$ (‰, V-PDB)	$\delta^{18}O$ (‰, V-PDB)	Δ_{47} (‰)	SD Δ_{47} (‰)	SE Δ_{47} (‰)	T (°C)	SE, T (°C)	$\delta^{18}O_{water}$ (‰) (V-SMOW), $T = T$ (Δ_{47})	Total Error $d^{18}O_{water}$ (‰), $T = T$ (Δ_{47})	$\delta^{18}O_{water}$ (‰) (V-SMOW), $T = 38$ °C
Alaska, U.S.A. (65.0, −147.3)	UAMES-4588 (bone)	Eolian	Pleistocene	2	−9.9	−16.3	0.643	0.013	0.009	37.8	2.2	−10.4	0.6	−10.4
Alaska, U.S.A. (65.5, −157.6)	UAMES-2067 (bone)	Fluvial	Pleistocene	2	−13.6	−13.6	0.693	0.013	0.009	26.4	2.0	−10.8	0.6	−7.7
Alaska, U.S.A. (65.5, −157.6)	UAMES-2180 (bone)	Fluvial	Pleistocene	3	−12.8	−11.2	0.714	0.018	0.011	21.9	2.2	−9.7	1.1	−5.3
Alaska, U.S.A. (66.3, −161.4)	UAMES-4517 (bone)	Eolian	Pleistocene	3	−12.8	−14.8	0.667	0.013	0.008	32.2	1.7	−10.5	0.6	−8.9
South Dakota, U.S.A. (43.4, −103.5)	10FG376 (bone)	Sinkhole	Pleistocene	3	−7.9	−11.4	0.696	0.013	0.008	25.9	1.6	−8.7	0.8	−5.5
South Dakota, U.S.A. (43.4, −103.5)	10FG489 (ivory)	Sinkhole	Pleistocene	2	−7.1	−10.4	0.703	0.013	0.009	24.2	1.9	−8.2	0.8	−4.5
South Dakota, U.S.A. (43.4, −103.5)	79HS173D (ivory)	Sinkhole	Pleistocene	3	−7.7	−9.0	0.694	0.014	0.008	26.2	1.6	−6.2	0.5	−3.1
Kansas, U.S.A. (39.1, −94.9)	KMNH-88518 (bone)	Fluvial	Pleistocene	2	−13.6	−2.7	0.655	0.030	0.021	35.0	5.0	2.5	2.4	3.3
Kansas, U.S.A. (unknown)	KMNH-119664 (bone)	Fluvial	Pleistocene	2	−10.1	−4.0	0.664	0.013	0.009	33.0	2.1	0.6	0.6	2.0
Kansas, U.S.A. (39.1, −94.9)	KMNH-97035 (bone)	Fluvial	Pleistocene	3	−11.0	−4.1	0.697	0.013	0.008	25.6	1.6	−1.5	0.6	1.8
Florida, U.S.A. (27.0, −82.1)	MBS_PL-FL-1 (bone)	Unknown	Pleistocene	3	−5.0	1.4	0.663	0.025	0.015	33.2	3.4	6.1	1.7	7.4
Elandsfonetein, S. Africa (−33.1, 18.2)	SA-Elndf-12871 (bone)	Coastal eolian	Pleistocene	3	−10.6	1.0	0.672	0.013	0.008	31.0	1.7	5.1	0.9	7.0
Elandsfonetein, S. Africa (−33.1, 18.2)	SA-Elndf-12897 (bone)	Coastal eolian	Pleistocene	3	−11.0	0.2	0.664	0.013	0.008	33.0	1.7	4.9	0.7	6.2
Nebraska, U.S.A.	UNSM-122060 (dentine)	Fluvial	Pliocene	3	−6.4	−6.3	0.716	0.031	0.018	21.6	3.7	−4.8	1.5	−0.4
Nebraska, U.S.A. (42.34, −98.24)	UNSM-1286-89B (dentine)	Fluvial	Pliocene	2	−6.1	−7.4	0.728	0.013	0.009	19.2	1.9	−6.7	0.6	−1.5
Chinese Loess Plateau (39.0, 111.2)	YJG-01 (dentine)	Eolian/paleosol	Miocene	2	−8.6	−4.9	0.668	0.013	0.009	32.0	2.1	−0.6	0.6	1.0
Chinese Loess Plateau (39.0, 111.2)	BDB-122 (dentine)	Eolian/paleosol	Miocene	3	−8.9	−6.4	0.675	0.013	0.009	30.4	2.1	−2.5	0.6	−0.5
Fayum Depression, Eygpt	BQ-2 (bone)	Fluvial	Eocene	3	−6.6	−1.1	0.644	0.015	0.009	37.7	2.1	4.8	0.7	4.9
Fayum Depression, Eygpt	L-30 (bone)	Fluvial	Oligocene	2	−15.0	−6.3	0.618	0.013	0.009	44.0	2.4	1.1	0.6	−0.4
Wyoming, U.S.A. (44, −108)	WWFm-4 (bone)	Fluvial/paleosol	Eocene	3	−16.9	−11.4	0.641	0.016	0.009	38.5	2.3	−5.4	0.8	−5.5
Wyoming, U.S.A. (44, −108)	WWFm-5 (bone)	Fluvial/paleosol	Eocene	2	−12.1	−16.0	0.611	0.013	0.009	46.0	2.4	−8.1	0.7	−10.2
Utah, U.S.A. (38.72, −109.86)	CMF-DW-Fem (bone)	Debris flow	Cretaceous	3	−6.4	−10.1	0.596	0.018	0.011	50.0	2.9	−1.2	1.1	−4.2
Utah, U.S.A. (38.72, −109.86)	CMF-DW-Fib (bone)	Debris flow	Cretaceous	2	−5.7	−10.6	0.591	0.013	0.009	51.4	2.5	−1.4	0.6	−4.7

N = the number of unique extractions of CO_2 from each sample. Δ_{47} values are reported on the carbon dioxide equilibrium scale described by Dennis et al., 2011. See Electronic Annex 1 for Δ_{47} values reported on the original Ghosh et al. (2006) scale, and Electronic Annex 2 for temperatures calculated using alternative calibrations. Temperatures were determined using the following equation: $\Delta_{47} = (0.0620 \times 10^6)/T^2 + 0.0021$, a revised equation by Eagle et al. (2013), where T is in Kelvin. Water $\delta^{18}O$ values were determined using the equation defined by Lécuyer et al. (2010) for bone carbonate ($1000\ln\alpha = 25.19 \times 10^3/T - 56.47$), where T is in Kelvin. Standard error (SE) is calculated from the standard deviation (SD) of N divided by the square root of N. Temperature SE is determined from the error in Δ_{47}. The total error in $\delta^{18}O$ of water is calculated based on the temperature error and error in $\delta^{18}O$ of carbonate, propagated through the Lécuyer et al. (2010) equation.

and Kraus, 1988; Seiffert, 2006). Two samples of fossil bone (WWfm-4, WWfm-5) were selected from the Eocene Willwood Formation, Wyoming, U.S.A., representing a fluvial depositional system with numerous well-developed paleosols (Bown and Kraus, 1993). Tooth dentine was sampled from the Big Springs Quarry (UNSM 1286-89B) and Quinn Gravel Pit (UNSM 122060), both part of the high-energy fluvial Broadwater Formation (Pliocene), Nebraska (Rogers, 1984; Swinehart et al., 1985; Passey et al., 2002; Duller et al., 2012). Finally, two tooth dentine samples (YJG-01; BDB-122) are from the Baode Formation of the Chinese Loess Plateau, a late Miocene sequence of stacked paleosols developed in eolian loess, with minor fluvial reworking (Zhu et al., 2008; Kaakinen et al., 2013).

3. METHODS

Bone, dentine, and cementum samples were cleaned of surrounding matrix with a toothbrush and ultrasonic bath under deionized water. Samples were dried in a low-temperature oven (~50 °C), and then crushed with a mortar and pestle. The resulting powder was then treated with hydrogen peroxide to oxidize organic contaminants and with acetic acid to dissolve labile and secondary carbonates, using methods outlined in Eagle et al. (2010), which follow the general approach of Koch et al. (1997). Eagle et al. (2010) explored the effects of progressively longer hydrogen peroxide treatment (3% solution) on measured Δ_{47} values of tooth enamel, and observed Δ_{47} values consistent with mammalian body temperature for reactions as short as 15 min and as long as 24 h. Samples that were not pretreated had anomalously low Δ_{47} values (=high apparent temperature), suggesting that hydrogen peroxide pretreatment is important, but that the precise duration of the pretreatment is not critical. Eagle et al. (2010) also systematically explored the effects of acetic acid treatment, subjecting four different materials (modern elephant enamel, elephant dentin, and fossil mammoth enamel and mammoth dentin) to four different treatments (no treatment, four hours in 0.1 M solution (pH = 2.8), 4 h in Na-acetate buffered 0.1 M solution (pH = 4.6), and 24 h in Na-acetate buffered 0.1 M solution (pH = 4.6)). The observed Δ_{47} values of samples subjected to these treatments generally conformed to body temperature (except for the fossil mammoth dentine, which gave a cooler apparent temperature consistent with low temperature diagenesis), although anomalous Δ_{47} values were observed for one sample receiving the pH 2.8 treatment, and for one sample receiving no treatment. Based on these results, Eagle et al. (2010) followed a 'preferred' pretreatment protocol consisting of 3% H_2O_2 (four hours, room temperature), followed by 0.1 M pH 4.6 acetic acid (4–24 h, room temperature).

We adopted this protocol, reacting sample powders in 3% H_2O_2 in a ratio of approximately 0.05 mL per 1 mg of bone powder, but reacting for 24 h in anticipation of higher organic contents of bone relative to the dentine and enamel studied by Eagle et al. (2010). The samples were rinsed in deionized water, and then treated with 0.1 M Na-acetate acetic acid solution buffered to a pH of 4.6. The solution was prepared by combining 2.8 g of Na-acetate and 2.9 mL of glacial acetic acid in deionized water to make 500 mL of solution. Bone samples were treated in a proportion of about 0.05 mL solution per 1 mg of bone, and allowed to react overnight at room temperature. After reactions, samples were rinsed three to five times in deionized water, centrifuging and decanting the supernatant between each rinse. Samples were then dried overnight at ~50 °C.

Carbonate comprises only a few weight percent of total bone (Elliott, 2002; Pasteris et al., 2008), so clumped isotope analyses require significantly more sample relative to what is required for pure calcite. For each analysis, we reacted approximately 110 mg of bone powder with 100% phosphoric acid. Use of our typical reaction temperature of 90 °C was problematic, resulting in over-vigorous reactions that ejected large amounts of sample powder from the acid bath, and that subsequently overflowed the heated area of the acid bath in a foamy mixture of acid and reaction product gases. Similar problems were observed by Eagle et al. (2010) in their attempts to analyze bioapatite samples using a similar common acid bath apparatus. The solution of Eagle et al. (2011) was to use a substantially larger acid bath to better contain the foamy reaction mixture. Our solution was to react samples at 25 ± 1 °C in McCrea-type glass reaction vessels, following methods of the original Caltech clumped isotope calibrations (e.g., Ghosh et al., 2006; Tripati et al., 2010; Thiagarajan et al., 2011). The much lower reaction temperature resulted in slower reactions and the elimination of the overflowing foamy reaction mixture. The reactions were carried out for 24 h, and held at constant temperature by immersion in a water bath. Following the reaction, the CO_2 was purified in an automated extraction line (Passey et al., 2010). Some of the experiments resulted in low CO_2 yields; it is suspected that the cause was leakage of the McCrea-type reaction vessels, and data associated with these experiments were discarded. Samples were analyzed in duplicate or triplicate as permitted by the amount of sample material available.

Calcium carbonates associated with pre-Quaternary bone samples were reacted in a common acid bath at 90 °C on the automated extraction line. The resulting CO_2 of the reactions was purified by passage through methanol-dry ice and liquid nitrogen traps (between which silver wool is placed as a getter for sulfurous gases), and then through a packed gas chromatograph column (PorapakQ) held at −20 °C. The CO_2 was analyzed for $\delta^{13}C$, $\delta^{18}O$ and Δ_{47} using a Thermo MAT 253 dual inlet mass spectrometer at Johns Hopkins University. The stable isotopic compositions of carbon and oxygen are reported relative to VPDB, and Δ_{47} values are reported relative to the absolute reference scale defined by Dennis et al. (2011), using an acid temperature correction of +0.092‰ (Henkes et al., 2013). A detailed description of our procedures for normalizing clumped isotope data relative to the scale of Dennis et al. (2011) is provided in Henkes et al. (2013). System stability was monitored both for the 25 °C reactions and the online 90 °C reactions by repeated analyses of in-house standards (UU-Carrara and 102-GC-AZ01): UU-Carrara at 90 °C, $\Delta_{47} = 0.407 \pm 0.017$ (mean ± 1σ), at 25 °C $\Delta_{47} = 0.399 \pm 0.014$ (mean ± 1σ);

102-GC-AZ01 at 90 °C, $\Delta_{47} = 0.699 \pm 0.014$ (mean $\pm$ 1σ), at 25° $\Delta_{47} = 0.706 \pm 0.015$ (mean $\pm$ 1σ).

Powder X-ray diffraction analysis of treated and untreated bone was performed at the Department of Geological Sciences at The University of Texas at San Antonio using a Scintag XDS 2000 XRD with a scan rate of 5° per minute from 2° to 70° 2θ.

4. RESULTS

4.1. Bioapatites

Table 1 summarizes the $\delta^{13}C$, $\delta^{18}O$, and Δ_{47} data acquired from both the Quaternary and pre-Quaternary samples, and Electronic Annex 1 provides raw and corrected isotopic data for each sample analysis. Alaskan bone samples have Δ_{47} values ranging from 0.643‰ to 0.714‰. Eagle et al. (2010) showed that bioapatites have virtually the same temperature–Δ_{47} relationship as calcite, and concluded that the Ghosh et al. (2006) paleotemperature equation is suitable for bioapatite. We use this equation, converted to the equilibrium reference frame of Dennis et al. (2011), as reported by Eagle et al. (2013, Table 4, therein). The Alaskan bone Δ_{47} values translate to $T(\Delta_{47})$ values ranging from 21.9 $\pm$ 2.2 °C for a mammoth rib fragment collected from the Koyukuk River, to 37.8 $\pm$ 2.2 °C for a rib fragment from the mummified bison "Blue Babe" (errors are given as 1 standard error, as reported in Table 1). South Dakota mammoths have Δ_{47} values ranging from 0.694 to 0.703‰ and $T(\Delta_{47})$ values ranging from 24.2 $\pm$ 1.9 °C to 26.2 $\pm$ 1.6 °C. This relatively small range comes from both bone and dentine (ivory) samples. Bones from Kansas have Δ_{47} values ranging from 0.655‰ to 0.697‰ and $T(\Delta_{47})$ values ranging from 25.6 $\pm$ 1.6 °C to 35.0 $\pm$ 5.0 °C. The Δ_{47} value of the single bone fragment analyzed from Florida is 0.663‰ corresponding to a $T(\Delta_{47})$ value of 33.2 $\pm$ 3.4 °C. The Δ_{47} of the two bone fragments from the Elandsfontein site, South Africa are 0.672‰ and 0.664‰, corresponding to a $T(\Delta_{47})$ value of 31.0 $\pm$ 1.7 °C and 33.0 $\pm$ 1.7 °C, respectively.

The two dentine samples from Pliocene sediments of the Broadwater Formation have Δ_{47} values of 0.728‰ and 0.716‰ corresponding to temperatures of 19.2 $\pm$ 1.9 °C to 21.6 $\pm$ 3.7 °C, respectively. Dentine samples from the Chinese Loess Plateau (Baode Formation; Miocene) have Δ_{47} values of 0.675‰ and 0.668‰ corresponding to a temperature of 30.4 $\pm$ 2.1 °C and 32.0 $\pm$ 2.1 °C, respectively. Bone fragments from the Willwood Formation (Eocene) have Δ_{47} values of 0.641‰ and 0.611‰ corresponding to a temperature of 38.5 $\pm$ 2.3 °C and 46.0 $\pm$ 2.4 °C, respectively. The bone fragment from the Birket Qarun Formation, Egypt (Eocene) has a Δ_{47} value of 0.644‰ and a $T(\Delta_{47})$ value of 37.7 $\pm$ 2.1 °C, and the bone fragment from the Jebel Qatrani Formation (early Oligocene) has a Δ_{47} value of 0.618‰ and temperature of 44.0 $\pm$ 2.4 °C. Finally, two bone fragments from the Cedar Mountain Formation (Cretaceous) have Δ_{47} values of 0.596‰ and 0.591‰ corresponding to a temperature of 50.0 $\pm$ 2.9 °C and 51.4 $\pm$ 2.5 °C, respectively.

The simultaneous measurement of $\delta^{18}O$ of carbonate and the Δ_{47}-derived temperature allows for the calculation of $\delta^{18}O$ of water ($\delta^{18}O_w$) associated with mineralization. Using the temperature dependent fractionation factor defined by Lécuyer et al. (2010) for the carbonate component of bone, water values relative to VSMOW were calculated for each bone sample. Quaternary bone samples from Alaska yield $\delta^{18}O_w$ values ranging from -10.8 ± 0.6‰ to -9.7 ± 1.1‰; from South Dakota ranging from -8.7 ± 0.8‰ to -6.2 ± 0.5‰; from Kansas ranging from -1.5 ± 0.6‰ to 2.5 ± 2.4‰; from Florida that average 6.2 ± 1.7‰; and from South Africa that range from 4.9 ± 0.7‰ to 5.1 ± 0.9‰. Pre-Quaternary bone from Pliocene sediments of the Broadwater Formation produced $\delta^{18}O_w$ values that range from −6.6‰ to −4.7‰; from the late Miocene Baode Formation that range from -2.5 ± 0.6‰ to -0.6 ± 0.6‰; from the Eocene Birket Qarun Formation and Jebel Qatrani Formation of the Fayum Depression that range from 1.1 ± 0.6‰ to 4.8 ± 0.7‰; from the Eocene Willwood Formation that range from -8.1 ± 0.7‰ to -5.3 ± 0.8‰; and from the Cretaceous Cedar Mountain Formation that range from -1.4 ± 0.6‰ to -1.2 ± 1.1‰.

4.2. Associated carbonates

In addition to bone carbonate analyses, we analyzed micritic crust and sparry calcite infill of bone from the Willwood Formation, carbonate horizons (interpreted as K or Bk horizons) from the Baode Formation, and carbonate nodules (interpreted as pedogenic carbonate nodules) from the Cedar Mountain Formation (Table 2). Temperatures were calculated using the calcite temperature–Δ_{47} relationship of Ghosh et al. (2006) as revised by Eagle et al. (2013). Oxygen isotopic compositions of waters associated with these calcites were determined based on the measured $\delta^{18}O$ of carbonate and $T(\Delta_{47})$ values using the equation for temperature dependent fractionation between calcite and water developed by Kim and O'Neil (1997). Baode Formation soil carbonate clumped isotope data are reported in Suarez et al. (2011), but four samples are reproduced here. These pedogenic carbonates have Δ_{47} values that range from 0.731‰ to 0.752‰ and produce $T(\Delta_{47})$ values ranging from 14.4 $\pm$ 1.4 to 18.6 $\pm$ 2.1 °C and $\delta^{18}O_w$ that ranges from -9.1 ± 0.3 to -8.2 ± 0.6‰ (VSMOW).

Carbonate samples from the Willwood Formation consist of micritic coatings on bone and sparry calcite infill of bone. Carbonates were analyzed from one of the bone samples that was also analyzed for Δ_{47} (WWFm-5). The micritic crust from this sample has a Δ_{47} value of 0.651‰ corresponding to a temperature and $\delta^{18}O_w$ value of 35.9 $\pm$ 2.2 °C, and -10.7 ± 0.4‰, respectively. The spar infill from this sample has a Δ_{47} value of 0.574‰ corresponding to a temperature and $\delta^{18}O_w$ value of 56.2 $\pm$ 2.0 °C, -11.4 ± 0.5‰, respectively. These compare with values from the bone itself of 46.0 $\pm$ 2.4 °C and -8.1 ± 0.7‰. Micritic crust and spar infill from an additional bone sample (itself not analyzed for Δ_{47}) was analyzed and produced similar temperatures to that of carbonates associated with WWFm-5: WWFm-6 micritic crust has a Δ_{47} value of 0.654‰, corresponding to temper-

Table 2
Stable carbon isotope, oxygen isotope, and clumped isotope data from calcites of pre-Pleistocene samples along with temperature and water isotopic composition.

Location	Sample name (type)	Period/ epoch	N	$\delta^{13}C$ (‰, V-PDB)	$\delta^{18}O$ (‰, V-PDB)	Δ_{47} (‰)	SD Δ_{47} (‰)	SE Δ_{47} (‰)	T (°C)	SE, T (°C)	$\delta^{18}O_{water}$ (‰) (V-SMOW)	SE $\delta^{18}O_{water}$ (‰)
Chinese Loess Plateau	CN2004-BD-117 (carbonate horizon)	Miocene	3	−7.1	−9.2	0.731	0.018	0.010	18.6	2.1	−8.2	0.6
Chinese Loess Plateau	CN2004-BD-124 (carbonate horizon)	Miocene	3	−6.8	−9.2	0.744	0.022	0.012	15.9	2.4	−8.7	0.7
Chinese Loess Plateau	CN2004-BD-141 (carbonate horizon)	Miocene	3	−6.9	−9.2	0.750	0.013	0.008	14.7	1.4	−8.9	0.4
Chinese Loess Plateau	CN2004-BD-162 (carbonate horizon)	Miocene	3	−6.5	−9.2	0.752	0.005	0.008	14.4	1.4	−9.1	0.3
Wyoming, U.S.A.	WWFm-6 (micritic crust)	Eocene	2	−10.2	−14.2	0.654	0.006	0.009	35.5	2.2	−9.8	0.5
Wyoming, U.S.A.	WWFm-6 (spar infill)	Eocene	3	−13.6	−17.6	0.578	0.007	0.008	54.9	1.8	−9.8	0.4
Wyoming, U.S.A.	WWFm-5 (spar infill)	Eocene	3	−12.0	−19.4	0.574	0.016	0.008	56.2	2.0	−11.4	0.5
Wyoming, U.S.A.	WWFm-5 (micritic crust)	Eocene	2	−10.0	−15.2	0.651	0.001	0.009	35.9	2.2	−10.7	0.4
Utah, U.S.A.	NAS-37 (carbonate nodule)	Cretaceous	2	−5.1	−8.2	0.659	0.007	0.009	34.0	2.1	−4.0	0.4

N = the number of unique extractions of CO_2 from each sample. Δ_{47} values are reported on the carbon dioxide equilibrium scale described by Dennis et al. (2011). See supplemental data for Δ_{47} values reported on the original Ghosh et al. (2006) scale. Temperatures were determined using the following equation: $\Delta_{47} = (0.0620 \times 10^6)/T^2 + 0.0021$, a revised equation by Eagle et al. (2013), where T is in Kelvin. Water $\delta^{18}O$ values were determined using the equation defined by Kim and O'Neil (1997): $1000\ln a = (18.03 \times 10^3)/T - 32.42$, where T is in Kelvin. All other values are reported as described in the footnotes of Table 1.

ature and $\delta^{18}O_w$ values of 35.5 ± 2.2 °C, and -9.8 ± 0.5‰, and sparry calcite infill has a Δ_{47} value of 0.578‰ corresponding to a temperature of 54.9 ± 1.8 °C, and $\delta^{18}O_w$ of -9.8 ± 0.4‰. A single carbonate nodule from the Cedar Mountain Formation was analyzed to compare to the Dalton Well's bone samples. The carbonate nodule was sampled from the same member as the Dalton Well's bone sample (Yellow Cat Member), but from a locality about 25 km northwest of the Dalton Well's locality. The Δ_{47} value for this sample is 0.659‰, corresponding to temperature and $\delta^{18}O_w$ values of 34.0 ± 2.1 °C, and -4.0 ± 0.5‰, respectively.

5. INTERPRETATIONS

5.1. Quaternary bone

5.1.1. Clumped isotopes

It is generally assumed that temperatures during shallow early diagenesis are similar to mean annual temperature (MAT) (Kohn and Law, 2006). However, bones fossilized near the surface in an environment influenced by pedogenesis (potentially the loess-deposit and coastal dune deposit environments studied here) may, like soil carbonates, produce $T(\Delta_{47})$ values that tend to be biased toward warm season temperatures, especially in temperate to high latitudes with high seasonality (Passey et al., 2010; Quade et al., 2013). We therefore compare the diagenetic $T(\Delta_{47})$ value of Quaternary bone to both the present day MAT and MWST (mean warm season temperature) of each locality, recognizing that temperatures during the late Quaternary were likely lower for some of the localities and that the latitudinal temperature gradient was probably steeper compared to the present day.

Fig. 2 displays clumped isotope derived temperatures from Quaternary bone carbonate, plotted as a function of absolute latitude. Also plotted are the MAT and MWST for each of the localities from which the Quaternary bone was recovered. It is immediately evident that the $T(\Delta_{47})$ of Quaternary bone and dentine samples reflect neither MAT nor MWST. The widest range of temperatures is observed for the bone samples from Alaska. The mummified bison bone sample with $T(\Delta_{47}) = 38 \pm 2$ °C suggests that the exceptional preservation of this specimen extends to preservation of original bone carbonate bond ordering. The non-mummified bones reveal a range of cooler temperatures, the coolest of 21.9 °C from a mammoth rib fragment recovered from river gravels of the Koyukuk River, a temperature that is still above MWST for this area.

The range of values from fossilized Alaskan bone suggests that the bone experienced partial recrystallization or contains a mixture of recrystallized and original carbonate. This may indicate that the samples analyzed are in varying stages of fossilization. To evaluate this possibility, samples were analyzed using powder XRD to qualitatively examine

the crystallinity of the bone, with the expectation that more extensively fossilized bone would have sharper and more intense peaks than pristine bone, reflecting greater crystallinity (e.g., Ayliffe et al., 1994). In particular, poorly-crystalline bone shows a broad peak between about 31–35° (2θ), and this feature sharpens into three or more distinct peaks with increasing crystallinity (Wheeler and Lewis, 1977; Bonar et al., 1983; Ayliffe et al., 1994; Correa de Araujo et al., 2011). The Alaskan samples showed very weak and broad peaks, with the mummified sample showing the broadest and least intense peaks (Fig. 3), consistent with minimal recrystallization of this sample.

Bone and dentine from the Mammoth Site in South Dakota also reflect incomplete resetting of clumped isotopes. Temperatures derived from these bones are close to, but just above mean warm season temperatures for South Dakota. The bone assemblage at the Mammoth Site is from a sinkhole accumulation in a karst region, and thus the diagenetic temperatures might be expected to approach MAT rather than WMMT. However, Laury (1980) tentatively suggest that the spring may have been fed by warm, hydrothermal waters. The XRD analysis of bone from the Mammoth Site show low intensity peaks, but with sharper features than those from the Alaska sites (Fig. 3), suggesting more extensive recrystallization.

Of the samples from Kansas (all recovered from Kansas River fluvial deposits) one has $T(\Delta_{47})$ indistinguishable from MWST, while the other two are ~5–10 °C warmer than MWST. The XRD scans of the sample that approaches MWST shows somewhat sharper XRD peaks for apatite than the others, suggesting that the sample was more extensively fossilized than those yielding higher apparent temperatures. The $T(\Delta_{47})$ values of bone samples from Elandsfontein, South Africa, are warmer than MWST, suggesting that the fossilization environment at Elandsfontein allowed for partial preservation of the original body temperature clumped isotope signature. These are the oldest Quaternary bones that were analyzed, so it was expected that clumped isotope temperatures should be more extensively equilibrated with MAT or MWST. The XRD scans show distinguishable, albeit low intensity, peaks. Likewise, the sample from Florida shows clear apatite peaks, though it produced a clumped isotope temperature warmer than modern MWST. These results suggest that the samples were only partially reset with respect to Δ_{47}, or that the temperatures of shallow subsurface fossilization environments during the Pleistocene were warmer than present-day MWST.

Since the publication of the original Ghosh et al. (2006) clumped isotope paleotemperature equation, many new calibrations have been published, and several of these have significantly lower temperature sensitivity than the Ghosh equation (e.g., Dennis and Schrag, 2010; Eagle et al., 2013; Henkes et al., 2013). Recalculation of $T(\Delta_{47})$ values of the Quaternary bone using these equations (Electronic Annex 2) does not significantly change the interpretations presented above. For example, using the Dennis and Schrag (2010) equation (as recalculated for the equilibrium reference frame by Dennis et al., 2011), the lowest observed $T(\Delta_{47})$ in the Quaternary dataset of 21.9 °C becomes 19.6 °C (fossilized bone from Alaska), and the highest temperature of 37.8 °C becomes 47.8 °C (mummified bone from Alaska). The latter value is clearly inconsistent with mammalian body temperatures. It is also unlikely that these Pleistocene materials experienced high burial temperatures, especially in the frozen substrate from which Blue Babe was recovered. This would suggest that the Dennis and Schrag (2010) equation is inappropriate for bioapatite, a conclusion supported by clumped isotope data from modern bone samples reported by Eagle et al. (2010). Thus the lack of conformance between $T(\Delta_{47})$ values of Quaternary bone and MAT or MWST is not attributable to an inappropriate calibration equation, at least in the context of what is presently known about the relationship between Δ_{47} and temperature in different minerals.

It is possible that our pretreatment procedures did not completely remove organic material from the bioapatite samples, resulting in spurious measurements of Δ_{47}, and indeed the broad XRD traces of many of the samples are consistent with the presence of organic carbon. Organic compounds could react during acid digestion to produce isobars that could interfere with the Δ_{47} analysis. However, such isobaric interference is commonly manifested in Δ_{48} values that deviate strongly from 0 (>±1‰) (Eiler and Schauble, 2004; Huntington et al., 2009). We observe no large anomalies in Δ_{48} (Electronic Annex 1), suggesting that our gas analytes were largely free of isobaric contaminants.

Mixing of materials with distinct bulk isotopic compositions ($\delta^{13}C$, $\delta^{18}O$) can produce mixtures with anomalous Δ_{47} values (Eiler and Schauble, 2004). As a hypothetical example, if diagenetically-altered bone contains a 50:50 mixture of 'primary' bone ($\delta^{13}C = -10‰$, $\delta^{18}O = -15‰$), and 'diagenetic' bone ($\delta^{13}C = 0‰$, $\delta^{18}O = -5‰$), the

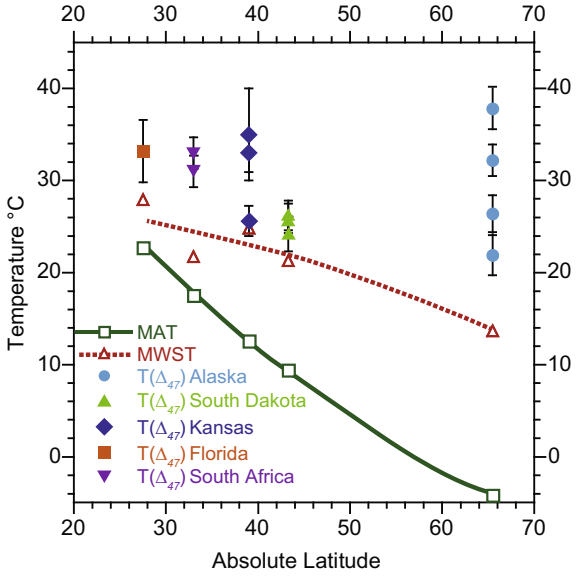

Fig. 2. $T(\Delta_{47})$ results from Quaternary bone (filled symbols), plotted as a function of absolute latitude, and compared with modern mean annual temperature (MAT; open squares) and mean warm season temperature (MWST; open triangles) of each study location (climate data from NOAA, 2013).

resulting mixture would have a Δ_{47} value that is 0.025‰ higher than the weighted mean Δ_{47} value of the primary and diagenetic components. For Earth surface materials, such mixing will generally lead to mixtures with higher Δ_{47} values than the starting materials (=lower apparent temperature). Thus, mixing effects are not a viable explanation for Δ_{47} values of Quaternary bone that are lower than would be expected for equilibrium at MAT or MWST.

5.1.2. Oxygen isotopes

The oxygen isotope data also provide insight into the extent of isotopic alteration of the bone samples. It is not uncommon for mammalian body water to be enriched in ^{18}O by several per mil relative to local meteoric water, due to intake of evaporated water (including leaf water), evaporation of water from the animal, and the influence of atmospheric O_2 ($\delta^{18}O \approx +23.5$‰), which contributes to body water via metabolism (Kohn,1996; Ayliffe and Chivas, 1990; Levin et al., 2006). This ^{18}O-enriched composition should be erased in bone that attains isotopic equilibrium with unevaporated soil and groundwater. Fig. 4 compares the apparent $\delta^{18}O$ of water ($\delta^{18}O_w$, calculated from bone carbonate $\delta^{18}O$ and $T(\Delta_{47})$ as described in Section 4.1) with mean annual $\delta^{18}O$ of precipitation as modeled by Bowen and Wilkinson (2002) as well as ranges for precipitation $\delta^{18}O$ from either Global Network for Isotopes in Precipitation (GNIP), Harris et al., 2010 (South Africa precipitation), or USNIP sources (Vachon et al., 2010). The majority of bone-derived $\delta^{18}O_w$ values are several per mil higher than meteoric water (as much as ~+7‰), consistent with incomplete oxygen isotope exchange between groundwater and bone carbonate. Only the Mammoth Site samples are within the range of meteoric $\delta^{18}O$ reported for that area (Vachon et al., 2010). With this exception, calculated $\delta^{18}O_w$ from bone carbonate are also more enriched than seasonal highs in $\delta^{18}O$ of precipitation (Fig. 4) indicating that seasonal differences do not account for this offset.

It is possible that part of this offset is related to exchange with evaporatively enriched groundwater, or seawater (in the case of the Florida sample found in coastal/inter-coastal areas). However, the consistently high absolute $\delta^{18}O$ values, primarily continental depositional environments, and several per mil magnitude of enrichment relative to meteoric water of many of the samples (e.g., samples from South Africa, Florida, and Kansas) are difficult to explain without invoking elevated $\delta^{18}O$ of body water.

In evaluating diagenesis of dinosaur enameloid, Eagle et al. (2011) discussed changes in $\delta^{18}O$ and Δ_{47} with regard to burial diagenesis and suggested that bulk $\delta^{18}O$ may be preserved during quasi-closed-system recrystallization in which the bond ordering is reset to reflect higher temperatures, but oxygen does not exchange significantly with diagenetic fluids. More generally, recrystallization in mineral-buffered systems (high rock to water ratio) will lead to resetting of ^{13}C–^{18}O bonds and minimal change in $\delta^{18}O$ (Dennis and Schrag, 2010; Eiler, 2011). Similarly, it may be possible that ^{13}C–^{18}O bonds in our Quaternary samples have partially reset at lower temperatures, but $\delta^{18}O$ of bone is largely reflective of the primary body water composition.

Values of $\delta^{18}O_w$ can be recalculated for the end-member scenario of no alteration of $\delta^{18}O_{bone}$. Under this scenario, the mineralization temperature relevant to oxygen isotopes is the original mammalian body temperature, 38 °C. The mineral–water fractionation factor at 38 °C is 1.0248, compared with a value of 1.0293 at 22 °C (Lécuyer et al., 2010), the lowest $T(\Delta_{47})$ observed in our bone dataset. Therefore, when calculated using $T = 38$ °C, the calculated $\delta^{18}O_w$ values are up to 4.5‰ higher than when calculated using $T = T(\Delta_{47})$ (Table 1). These values are significantly higher than estimated values of meteoric waters in each study location, but are still plausible values for body water.

5.2. Pre-Quaternary bone

Fig. 5 plots the $T(\Delta_{47})$ for pre-Quaternary bone samples versus estimates of maximum burial temperature. These estimates of maximum burial temperature are taken from the literature, or calculated based on estimates of the maximum burial depth multiplied by an average geothermal gradient of 25° C/km, with information drawn from the following references: Fayum Depression, Egypt: Kappelman et al. (1992); Broadwater Formation, Nebraska, USA: Diffendal (1995); Willwood Formation, Wyoming, USA: Bao et al. (1998); Baode Formation, Shanxi, China: Zhu et al. (2008); Cedar Mountain Formation, Utah, USA: Hintze (1993), Neuendorf et al. (2005). Also plotted are the $T(\Delta_{47})$ for micrite and/or spar in nodules or coatings where present (Baode Formation, Willwood Formation and Cedar Mountain Formation). For the youngest samples (Miocene and Pliocene samples), the burial depths were shallow and maximum burial temperatures did not exceed mammal body temperature. Dentine samples from the Broadwater Formation produced the coolest temperatures (19.2 °C and 21.6 °C). Samples (dentine) of Miocene age from the Baode Formation produce temperatures that are significantly warmer (30.4 °C and 32.0 °C) than coeval soil carbonates (average 18.2 °C; Suarez et al., 2011). The $T(\Delta_{47})$ of dentine from the Baode Formation either reflects a contribution of original mammal body temperature or is more reflective of early diagenesis at peak warm season soil temperatures than are the associated soil carbonates. If this is the case, these temperatures are greater than modern MWST (20 °C), but would be consistent with a warmer Mio-Pliocene climate. Calculated $\delta^{18}O_{water}$ values from bone and coeval soil carbonates suggests that the two carbonate phases were precipitated from water with different $\delta^{18}O$ compositions. The pedogenic carbonates (averaging −8.7‰) are lighter than the bone carbonate (averaging −1.5‰). Because mammal body water is typically more enriched in ^{18}O than meteoric water, this could be interpreted as an original biogenic $\delta^{18}O$ value in bone carbonate, and could suggest relatively closed-system recrystallization leading to incomplete equilibration of oxygen isotopes with soil water, but leading to significant changes in clumped isotope compositions. Alternatively, the bone carbonate may have equilibrated with early diagenetic fluids with different isotopic compositions and temperatures than those responsible for soil carbonate mineralization.

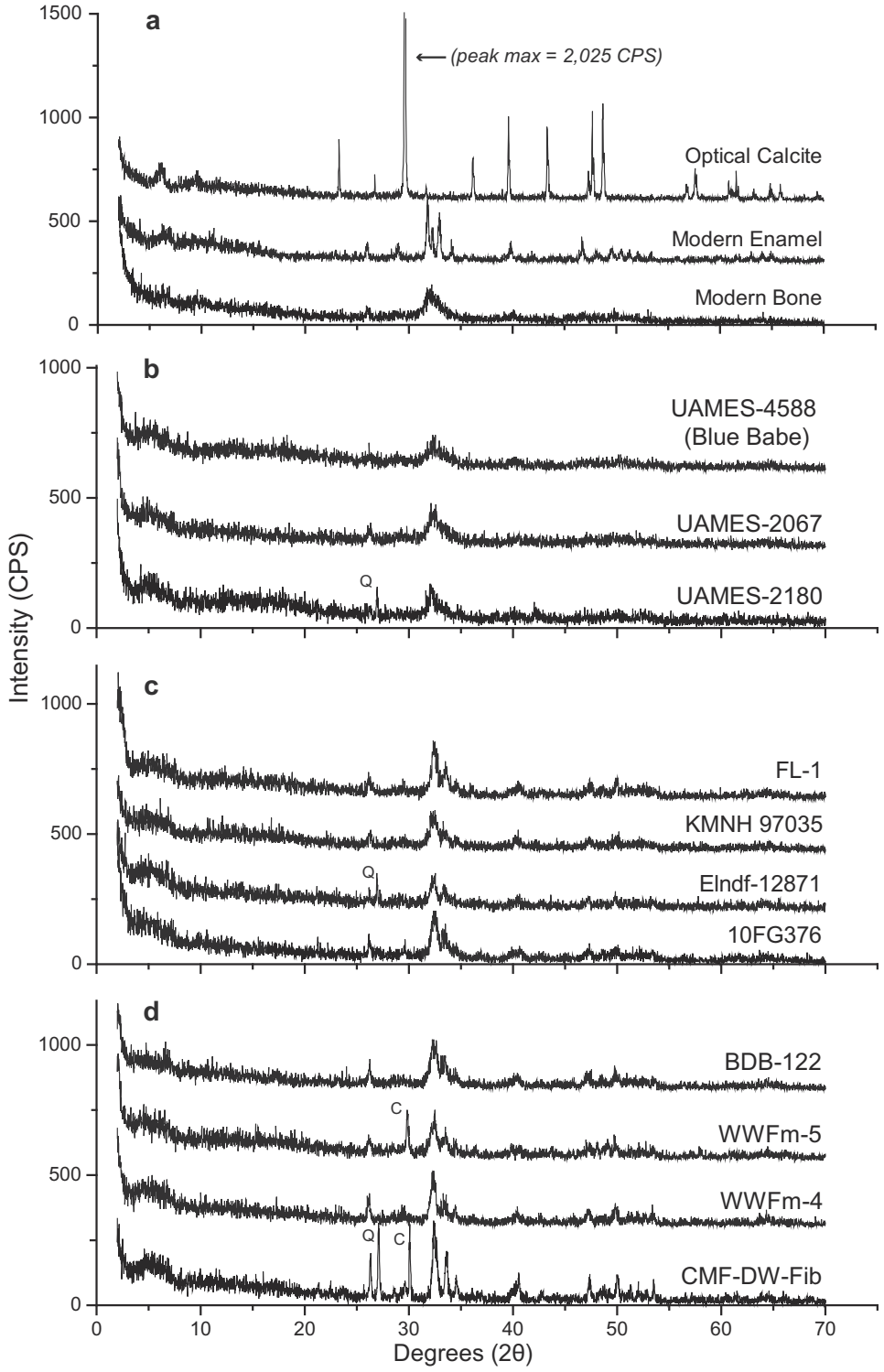

Fig. 3. XRD analyses of bone and mineral samples. (a) Representative traces of optical calcite, modern enamel (rhinoceros), and modern bone (elk). (b) Traces of representative samples from Alaska. These bones show broadly defined peaks similar to the modern bone (especially the bone from the mummified bison "Blue Babe"). (c) Representative Quaternary bone samples. (d) Representative pre-Quaternary bone samples. These samples show well-defined peaks reflecting greater crystallinity. "C" represents calcite peaks found in one of the Willwood Formation samples (WWFm-5) and the Cedar Mountain Formation samples. "Q" represents quartz peaks.

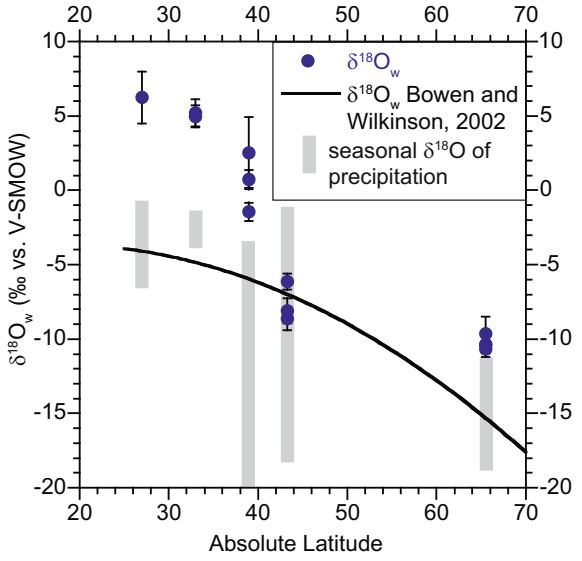

Fig. 4. Apparent oxygen isotopic composition of water in equilibrium with bone carbonate (vs. VSMOW) calculated based on Quaternary bone carbonate $\delta^{18}O$ and $T(\Delta_{47})$. Solid line represents a modern global latitudinal gradient of mean annual $\delta^{18}O$ of meteoric water, based on the model of Bowen and Wilkinson (2002). Gray bars show the observed ranges in $\delta^{18}O$ of precipitation for each locality based on data from the IAEA (2013) for Alaska (Bethel, Alaska) and South Africa (also including data from Harris et al., 2010), and from Vachon et al. (2010) for South Dakota, Kansas and Florida. Note that these ranges likely underestimate the full range in $\delta^{18}O$ of precipitation at many of the localities, given the limited number of observations.

Paleogene aged samples from the Fayum Depression of Egypt (Birket Qarun and Jebel Qatrani Formations) and the Willwood Formation in Wyoming, U.S.A. give a range of $T(\Delta_{47})$ values that are at the upper limits of recorded modern soil temperatures (approximately 35–40 °C at depths >50 cm) and in a range that could also be interpreted as resetting during burial diagenesis (greater than ~40 °C; Quade et al., 2013). Given that mammal bone from these localities would initially reflect mammal body temperature of ~38 °C, it is difficult to distinguish among body temperature, an early diagenetic alteration in a warm soil environment, and later burial diagenesis at elevated temperatures. The bone sample WWFm-5 (Willwood Formation) from which both a micritic coating and sparry calcite infill were analyzed, provided a range of temperatures. The clumped isotope temperature of sparry calcite (56.2 °C) approaches, but does not reach, an estimated maximum burial temperature of ~70 °C (Bao et al., 1998). However, this Δ_{47} value is sufficiently low that it may be outside of the range of the Ghosh et al. (2006) calibration, and use of the Guo et al. (2009) theoretical calibration, as recast on the equilibrium scale (Passey and Henkes, 2012, Eq. (4)), gives a calculated $T(\Delta_{47})$ of 67 °C, which is indistinguishable from the estimated maximum burial temperature of 70 °C. Clumped isotope analysis of the micritic coating of this sample gives a lower temperature of 35.9 °C (approaching warmest modern soil temperatures). The bone carbonate of this sample gives a temperature that is between these two end members (46.0 °C).

These observations lead to the suspicion that not all of the diagenetic calcite was removed with the 0.1 M acetic acid treatment. Analysis of this sample using powder XRD reveals a small (relative to the untreated sample) but recognizable peak diagnostic for calcite at $2\theta = 29.4°$. When compared to published values from the same approximate stratigraphic level, the $\delta^{18}O_{CO3}$ of bone and micrite (−16.0‰ to −11.4‰ VPDB) overlaps with values for fracture-filled sparry calcite in nodules reported by Bao et al. (1998) (−17.7‰ to −13.1‰ VPDB), consistent with the bone sample containing some amount of late diagenetic calcite and/or with the bone carbonate and micritic crust having experienced partial burial recrystallization.

A second bone sample (WWFm-4) gave $T(\Delta_{47})$ similar to the micritic values of WWFm-5 and micritic crust from a different bone. This particular sample (a crocodile scute) comes from the Paleocene-Eocene transition level of the Willwood Formation and the resulting temperature (38.5 °C) is somewhat warm, but not implausible for ground temperatures during this warm period in Earth history (e.g., VanDeVelde et al., 2013). The XRD scan of this

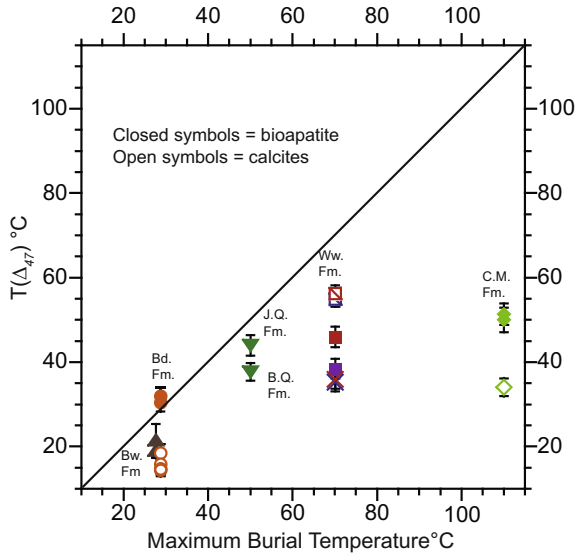

Fig. 5. Maximum burial temperature versus $T(\Delta_{47})$ for pre-Quaternary bone samples and calcites. Maximum burial temperature estimates are taken from the literature (Bao et al., 1998) or are calculated based on the thickness of overlying strata and assuming an average geothermal gradient of 25 °C/km (Neuendorf et al., 2005). Closed symbols are bone carbonates. Open symbols are calcites. For the Willwood Formation, squares with single diagonal are sparry calcite infilling bone, while × symbols are micritic crusts on bone. Red symbols are WWFm-5, Purple square is WWFm-4, Blue symbols are WWFm-6. Bw. Fm. = Broadwater (gray triangles); Bd. Fm. = Baode Formation (orange circles); B.Q. Fm. = Birket Qarun Formation; J.Q. Fm. = Jebel Qatrani Formation (green inverted triangles); Ww. Fm. = Willwood Formation (squares and × symbols); and C.M. Fm. = Cedar Mountain Formation (green diamonds). (For interpretation of the references to color in this figure legend, the reader is referred to the web version of this article.)

sample showed no calcite peaks, so the high $T(\Delta_{47})$ value cannot be attributed to contamination by a late phase of calcite. Generally, it is difficult to discern whether the temperatures from the bone and micritic samples represent partial reordering of bonds due to burial diagenesis, or early diagenetic soil temperatures. The Eocene Willwood Formation is known to have been deposited in an equable climate, warmer than climates in present-day Wyoming (Bown and Kraus, 1993; Bains et al., 2003; Fricke and Wing, 2004), and clumped isotope compositions of soil carbonates suggest that soils typically reached ~35 °C during at least part of the year (Snell et al., 2013). The $\delta^{18}O$ of water calculated from bone carbonate is elevated (averaging −6.7‰) relative to values calculated from the micritic and sparry calcite phases (averaging −10.4‰). As with the Baode Formation this could be interpreted as a contribution of the original body water composition, or variability in the diagenetic fluids to which the bones were subjected. Considering the age of the bone, it seems unlikely that the $\delta^{18}O$ of bone carbonate could retain original $\delta^{18}O$ values, and so this enriched value probably represents an enriched end-member of early diagenetic $\delta^{18}O$ water values.

The oldest samples analyzed are bone fragments from a sauropod femur and tibia from the Lower Cretaceous Cedar Mountain Formation in eastern Utah. Based on the thickness of the overlying sedimentary sequence, the unit experienced temperatures up to ~110 °C (assuming a geothermal gradient of 25° C/km). The $T(\Delta_{47})$ values are 50 °C and 51 °C (or 57 and 59 °C using the Guo et al. (2009) calibration), suggesting that either bone carbonate bond ordering was not completely reset, or that complete resetting occurred, but that the bone recrystallized at a lower temperature as the Cedar Mountain Formation was exhumed. XRD analyses of the bone samples indicate that the CMF samples contain a small amount of calcite that was not removed during the acetic acid treatment. It is therefore possible that the bioapatite-bound carbonate may record a different temperature, but observation of such a signal would require development of more specialized pretreatment procedures capable of removing all authigenic calcite without causing recrystallization of the bioapatite. Clumped isotope analysis of a single soil carbonate nodule from the Cedar Mountain Formation approximately 25 km from the Dalton Wells Site provides a temperature estimate of 34 °C. Like the WWFm-4 and micritic crusts from the Willwood Formation, the CMF soil carbonate temperature estimate is close to the maximum observed globally for present-day soil temperatures at depths below the surface greater than about 50 cm. Also, like the Eocene Willwood Formation, the Cretaceous Cedar Mountain Formation climate was likely much warmer than today, and ground surface temperatures may have been higher than those expected for modern soils.

The $\delta^{18}O_{water}$ values for both the carbonate nodule from the CMF and for the bone carbonate are enriched relative to present-day meteoric waters, with the $\delta^{18}O_{water}$ from bone carbonate being more enriched than the soil carbonate nodule (average −1.3‰ vs. −4.0‰). Considering the temperatures calculated from bone carbonate, it is possible that these values are related to deeper pore water, as $\delta^{18}O$ of pore waters can be elevated owing to diagenetic reactions at depth (Clayton et al., 1966; Savin, 1980; Fayek et al., 2001). The $\delta^{18}O_w$ value from the carbonate nodule (−4.0‰), while lower than this value is somewhat enriched considering the continental depositional environment. However, the upper Yellow Cat Member is interpreted to have been deposited in a semi-arid to arid climate, so it may also represent enrichment due to evaporation (Kirkland and Madsen, 2007). As an example, Breecker et al. (2009) report $\delta^{18}O$ soil water values as high as +1‰ (VSMOW) from modern shrublands of central New Mexico.

6. DISCUSSION AND IMPLICATIONS

The initial hypothesis that clumped isotope derived temperatures from Quaternary bone carbonate will record a temperature gradient similar to a modern ground temperature gradient is not supported by our data. Fig. 2 shows conclusively that clumped isotope derived temperatures of bone carbonate bear little to no resemblance to latitudinal temperature gradients of MAT or MWST. The majority of the bone carbonate analyses produce temperatures warmer than both MAT and MWST. The Blue Babe and the Mammoth Site bones date to the time of the Wisconsonian Glaciation, so it is unlikely that the paleotemperatures experienced by these samples were warmer than present-day temperatures. In general, the time-integrated climate of the late Pleistocene is thought to be cooler than the present-day climate, more so at high latitudes than low latitudes (e.g., Cuffey et al., 1995; Tierney et al., 2008), so it is difficult to invoke climate change as an explanation for the elevated diagenetic $T(\Delta_{47})$ values. Likewise, the majority of the $\delta^{18}O_w$ values derived from the clumped isotope analyses are more enriched than expected for equilibration with groundwater derived from meteoric waters. Late Pleistocene precipitation in mid- to high-latitudes should generally be lower in $\delta^{18}O$ than present day precipitation (Jouzel et al., 2000), so it is unlikely that the elevated values inferred from Pleistocene bone are an artifact of higher primary precipitation $\delta^{18}O$ values. Rather, they are interpreted to represent original body water compositions, or a combination of original body water and meteoric water compositions. It is not uncommon for body water $\delta^{18}O$ values to be several per mil higher than coexisting meteoric waters $\delta^{18}O$ values (e.g., Ayliffe and Chivas, 1990; Kohn, 1996; Levin et al., 2006). In the specific case of the Elandsfontein, South Africa samples, tooth enamel has similarly high $\delta^{18}O$ values as bone (up to ~+2‰; Luyt et al., 2000). Since tooth enamel is resistant to diagenesis, this provides a strong argument that the body water of these animals was elevated in ^{18}O relative to meteoric waters.

It is possible that the set of bone samples from which this conclusion is based experienced milder diagenesis than is typical for pre-Pleistocene fossil bone, despite having an outward appearance of being well fossilized. XRD analysis of the bone samples (Fig. 3) confirms that a number of the bones are poorly crystalline (particularly samples from Alaska), although many of the samples show fairly well defined XRD peaks. The Quaternary samples are generally

Table 3
Carbon and oxygen isotopic compositions of pairs of enamel and bone/dentine/cementum from the same fossil specimens from the late Miocene Baode Formation, Shanxi Province, China.

Sample ID	Locality	Family	Genus	Material	$\delta^{13}C$ (‰, V-PDB)	$\delta^{18}O$ (‰, V-PDB)
M7423	30	Rhinocerotidae	Chilotherium	Bone	−8.3	−4.5
				Enamel	−10.0	−4.0
M10405	114	Bovidae	Plesiaddax	Bone	−6.0	−2.5
				Enamel	−5.8	−4.4
BD.265.YJG03	YJG03	Equidae		Cementum	−7.0	−7.0
				Enamel	−8.1	−5.7
M3824	49	Equidae	Hipparion	Cementum	−6.4	−8.2
				Enamel	−8.8	−8.5
BD.261.YJG03	YJG03	Giraffidae	Samotherium	Dentine	−6.1	−5.0
				Enamel	−7.4	−10.0
BD.263.YJG03	YJG03	Giraffidae	Samotherium	Dentine	−6.6	−4.6
				Enamel	−8.1	−6.5
BD.278.YJG03	YJG03	Giraffidae	Samotherium	Dentine	−6.4	−6.0
				Enamel	−6.8	−6.5
BD.280.YJG03	YJG03	Equidae		Dentine	−7.7	−7.6
				Enamel	−8.8	−8.3
M11327	49	Bovidae	Gazella	Dentine	−10.4	−6.8
				Enamel	−11.9	−7.2
M11328	49	Bovidae	Gazella	Dentine	−7.3	−2.7
				Enamel	−9.0	0.1
M11320	30	Bovidae	Gazella	Dentine + bone	−9.8	−7.9
				Enamel	−11.8	−10.0

Locality information is given in Kaakinen et al. (2013). Stable isotope analyses were conducted at the University of Utah using a common acid bath extraction device (acid temperature 90 °C) coupled to a Finnigen MAT 252 mass spectrometer. Data are normalized to NBS-19 using concurrent analyze of in-house tooth enamel and calcite standards calibrated against NBS-19.

young (<50 ka), and many of them come from settings that would probably not be preserved over geological timescales (e.g., samples from loess deposits in Alaska, and the sinkhole deposits from South Dakota). The samples generally do not come from actively aggrading fluvial depositional systems with superimposed soils of the type studied by Kohn and Law (2006) and Zanazzi et al. (2007). It is possible that active pedogenesis, high soil pCO_2, and other aspects of such environments promotes isotope exchange between bone and pore fluids.

To further explore these issues, we examined a set of samples from late Miocene strata from the Chinese Loess Plateau. Specifically, we determined isotopic compositions ($\delta^{13}C$, $\delta^{18}O$) of 11 pairs of fossil mammal herbivore tooth enamel and bone (including dentine and cementum) from the late Miocene Baode Formation, a cumulative stack of paleosols formed in aggrading eolian loess with abundant soil carbonate nodules and horizons, and with minor fluvial reworking (Passey et al., 2009; Kaakinen et al., 2013). Each pair includes tooth enamel and bone, dentine, or cementum from the same fossil specimen. The tooth enamel should preserve primary $\delta^{13}C$ and $\delta^{18}O$ values of the animal, reflecting diet, behavior, and physiology, whereas the bone/dentine/cementum should merge to a common isotopic composition in the case of complete isotopic exchange with soil fluids (Kohn and Zanazzi, 2008). The range of carbon and oxygen isotopic values of these soil fluids are reflected by the range of soil carbonate values. The results are presented in Table 3 and Fig. 6. Tooth enamel shows the widest range in $\delta^{13}C$ and $\delta^{18}O$, reflecting browsing (C_3 plants; ^{13}C-depleted) and mixed-feeding ($C_3 + C_4$, ^{13}C-enriched) diets and a range of body water $\delta^{18}O$ values. The isotopic compositions of bone/dentine/cementum clearly converge toward, but never attain, a common value with $\delta^{13}C$ similar to soil carbonate in the same sections, and with $\delta^{18}O$ elevated by a few per mil relative to soil carbonate.

These data point to incomplete isotope exchange in the soil environment: both $\delta^{18}O$ and $\delta^{13}C$ of bone/dentine/cementum seem to partially record the original isotopic composition of the animal, and partially record conditions during diagenesis. It is uncertain why the apparent diagenetic $\delta^{18}O$ value is higher than the value recorded by paleosols. One possibility is that soil water had a different mean $\delta^{18}O$ value during bone diagenesis than during soil carbonate formation. Suarez et al. (2011) suggest that soil carbonates in these strata primarily formed during or especially after the warm, rainy season as soils became less saturated. Soil carbonates may have formed under a restricted set of environmental conditions (e.g., warm-season-biased formation, or formation during only short intervals of orbital cycles), whereas bone may have been subject to isotope exchange with soil waters during the full seasonal cycle and during all parts of the orbital cycle. Also, CO_2 released during decomposition of bone organic carbon, and unknown kinetic effects, may be additional factors leading to differences in bone carbonate and soil carbonate isotopic compositions. Regardless of the isotopic composition of diagenetic fluids during bone diagenesis, it is clear from Fig. 6 that bone samples converge toward a common com-

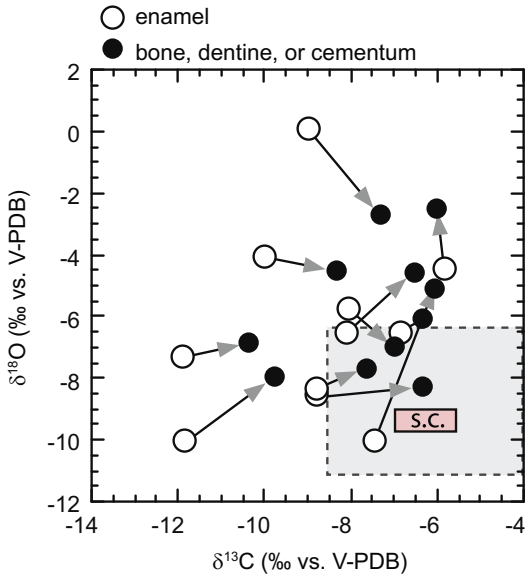

Fig. 6. Carbon and oxygen isotopic compositions of pairs of fossilized tooth enamel (open circles) and bone, dentine, or cementum ('BDC'; filled circles) from the late Miocene Baode Formation, Chinese Loess Plateau. Each pair comes from a single fossil specimen. The box labeled 's.c.' shows the average and standard deviation of ~160 soil carbonate analyses of samples collected from the same sections from which the fossils were collected, and the larger box bounded by a dashed line shows the total range of $\delta^{13}C$ and $\delta^{18}O$ of these carbonates (data from Passey et al., 2009). The BDC values converge toward a diagenetic isotopic composition with a carbon isotopic composition similar to soil carbonates, and with an oxygen isotopic composition a few per mil higher than soil carbonates. This figure is modified after Fig. 5 of Passey (2012).

position in $\delta^{13}C$ and $\delta^{18}O$, but that they fail to reach equilibrium with those compositions.

Based on this dataset, and the isotopic data from Quaternary bone, it is apparent that the isotopic composition of fossil bone variously records the original isotopic composition of the animal during bone growth, the isotopic composition of the environment of fossilization, and subsequent conditions during burial and exhumation of the fossil. The clumped isotope composition of the bone (with the exception of the mummified bone) has recognizably changed from its original bond ordering, but the $\delta^{18}O$ appears to have not yet equilibrated with early meteoric fluids even though the bone has an outward appearance of being fossilized. Indeed, a number of studies (Tütken, 2003; Tütken et al., 2004; Kocsis et al., 2010; Tütken et al., 2011) suggest that rate of fossilization can be highly variable and extend into geological time. In addition, Tütken (2003) and Tütken et al. (2004) suggest that some fossilization environments such as those in fine-grained sediments or permafrost may inhibit circulation of diagenetic fluids and thus water–rock (fossil) interaction. This scenario could plausibly be invoked for the Alaskan samples. It could explain the reordering of C–O bonds in carbonate without significant exchange in oxygen isotopic composition. Our study reinforces the idea that fossilization is a complex process and that the stable isotopic composition bioapatites is dependent on multiple factors including time, temperature, pore water chemistry, and water–rock ratios.

Interpretation of pre-Quaternary bone carbonate data is somewhat ambiguous. The calcite contamination of one of the Willwood Formation bones and the Cedar Mountain Formation bones prohibits a satisfying interpretation, and underscores a practical challenge: selective removal of contaminating phases without recrystallizing the bioapatite fraction. It is clear from this study is that the overnight 0.1 M acetic acid treatment of bone is not always sufficient to remove contaminating phases such as calcite, particularly for bone which has much greater porosity (easily pervaded by calcite) than enamel.

Eagle et al. (2011) analyzed bioapatites from near the Cedar Mountain Formation (CMF) location from the underlying Jurassic Morrison Formation in Utah, and found that samples exhibited different degrees of late diagenetic alteration. Of the three bioapatite phases analyzed, bone carbonate of the Morrison Formation produced temperatures that were cooler (between 50 °C and 60 °C, similar to our results) than dentine and enamel (~100 °C). It would appear that the bone and dentine responded to burial diagenesis somewhat differently than the enamel. The presence of calcite in the bone analyzed from the CMF precludes a direct comparison with the Eagle et al. (2011) results, but would suggest that the bone in the CMF may have experienced similar burial temperatures. The temperature calculated from the analysis of the CMF soil carbonate is a more reasonable temperature for earth surface conditions, and also suggests that different carbonate phases seem to respond differently to the initial depositional environment and subsequent deep burial and exhumation.

Observed $\delta^{18}O_w$ values also suggest that bone carbonate was often not completely re-equilibrated with early diagenetic waters. Nearly all of the Quaternary bone-derived $\delta^{18}O_w$ values are elevated compared to local meteoric water. Analysis of coeval soil carbonates and enamel from the Miocene Baode Formation indicates that this pattern also occurs in pre-Quaternary bone carbonate. Indeed, several studies (e.g., Tütken, 2003; Tütken et al., 2004; Piga et al., 2009; Kocsis et al., 2010; Tütken et al., 2011) suggest that fossilization can continue to occur into such time scales. Bone samples older than this are likely to reflect some degree of isotopic alteration, although we do not discount the possibility of preservation of original biogenic values in special circumstances such as mummification or other instances of superb preservation.

7. CONCLUSIONS

Clumped isotope analyses of bone carbonate from Quaternary to Cretaceous samples indicate that the clumped isotope thermometer applied to bone carbonate is capable of recording aspects of the original biology of the animal, early diagenesis, and later diagenesis during deep burial and exhumation. With the exception of mammoth bone and ivory samples from the Mammoth Site sinkhole accumulation in South Dakota and a bone fragment recovered from the Kansas River, Kansas, the Quaternary samples

produce $T(\Delta_{47})$ values that are much higher than modern mean annual temperature and modern mean warm season temperatures, indicating that apatite crystallites retain a component of original bond ordering within the carbonate. XRD analyses indicate that the partial retention of original bond ordering is probably a result of incomplete fossilization. Clumped isotope temperatures of bone and dentine samples predating the Quaternary provide ambiguous results which could be interpreted as either late burial diagenetic temperature, preservation of early diagenetic environments reflective of greenhouse climates, or contamination with diagenetic calcite not completely removed by pretreatment procedures. Lastly, the $\delta^{18}O$ of water calculated from $\delta^{18}O$ of carbonate and $T(\Delta_{47})$ support the idea that bone carbonate from samples as old as Miocene did not completely re-equilibrate with fluids in early diagenetic fossilization environment.

Despite these complications, the clumped isotope compositions of fossil bone may yet provide useful constraints on past ground temperatures. As a hypothetical example, an observation of $T(\Delta_{47})$ of fossil bone of 80 °C indicates that the bone and associated strata reached temperatures of 80 °C or higher. Similarly, a $T(\Delta_{47})$ of 15 °C observed for mammalian bone with a 38 °C initial temperature indicates that the bone reached temperatures of 15 °C or cooler at some point during fossilization. Such constraints are broad, but they may be useful in conjunction with other kinds of data relevant to burial temperatures, for example the clumped isotope compositions of other carbonate phases, fluid inclusion homogenization temperatures, and conodont color alteration indices.

ACKNOWLEDGEMENTS

Funding for this study was provided by the Morton K. Blaustein Postdoctoral Fellowship from the Department of Earth and Planetary Sciences at Johns Hopkins University. We wish to thank our colleagues who provided sample material: Dr. Kenneth Rose, Johns Hopkins University; Dr. Pat Druckenmiller and Julie Rousseau, Museum of the North at the University of Alaska, Fairbanks; Dr. Don Esker, the Mammoth Site, Hot Springs, South Dakota; Dr. Naomi Levin, Johns Hopkins University; Dr. James Kirkland, Utah Geological Survey; and Dr. Dan Burnham, Kansas Museum of Natural History. A special acknowledgement is given to the late Dr. Larry Martin, Kansas Museum of Natural History, for not only sharing material for analyses, but for sharing his diverse ideas and encouraging his students to always think outside the box. Finally, we thank the thoughtful comments provided by three reviewers including Dr. Matthew Kohn.

APPENDIX A. SUPPLEMENTARY DATA

Supplementary data associated with this article can be found, in the online version, at http://dx.doi.org/10.1016/j.gca.2014.05.026.

REFERENCES

Agenbroad L. D. (1989) Hot springs, South Dakota: entrapment and taphonomy of Colombian Mammoth. In *Quaternary Extinctions: A Prehistoric Revolution* (eds. P. S. Martin and R. G. Klein). The University of Arizona Press, p. 892.

Agenbroad L. D. (2005) North American proboscideans: mammoths: the state of knowledge, 2003. *Quat. Int.* **126–128**, 73–92.

Amiot R., Buffetaut E., Lecuyer C., Wang X., Boudad L., Ding Z., Fourel F., Hutt S., Martineau F., Medeiros M. A., Mo J., Simon L., Suteethorn V., Sweetman S., Tong H., Zhang F. and Zhou Z. (2010) Oxygen isotope evidence for semi-aquatic habits among spinosaurid theropods. *Geology* **38**, 139–142.

Ayliffe L. K. and Chivas A. R. (1990) Oxygen isotope composition of the bone phosphate of Australian kangaroos: potential as a paleoenvironmental recorder. *Geochim. Cosmochim. Acta* **54**, 2603–2609.

Ayliffe L. K., Chivas A. R. and Leakey M. G. (1994) The retention of primary oxygen isotope compositions of fossil elephant skeletal phosphate. *Geochim. Cosmochim. Acta* **58**, 5291–5298.

Bains S., Norris R. D., Corfield R. M., Bowen G. J., Gingerich P. D. and Koch P. L. (2003) Marine-terrestrial linkages at the Paleocene–Eocene boundary. In *Causes and Consequences of Globally Warm Climates in the Early Paleogene* (eds. S. L. Wing, P. D. Gingerich, B. Schmitz and E. Thomas). Geological Society of America, Boulder, CO, pp. 1–9.

Bao H., Koch P. L. and Hepple R. P. (1998) Hematite and calcite coatings on fossil vertebrates. *J. Sediment. Res.* **68**, 727–738.

Barrick R. E., Fischer A. G. and Showers W. J. (1999) Oxygen isotopes from turtle bone: applications for terrestrial paleoclimates? *Palaios* **14**, 186.

Bonar L. C., Roufosse A. H., Sabine W. K., Grynpas M. D. and Glimcher M. J. (1983) X-ray diffraction studies of the crystallinity of bone mineral in newly synthesized and density fractionated bone. *Calcif. Tissue Int.* **35**, 202–209.

Bowen G. J. and Wilkinson B. (2002) Spatial distribution of $\delta^{18}O$ in meteoric precipitation. *Geology* **30**, 315–318.

Bown T. and Kraus M. (1993) Time-stratigraphic reconstruction and integration of paleopedologic, sedimentologic, and biotic events (Willwood Formation, Lower Eocene, northwest Wyoming, USA). *Palaios* **8**, 68–80.

Bown T. M. and Kraus M. J. (1988) *Geology and paleoenvironment of the Oligocene Jebel Qatrani Formation and adjacent rocks, Fayum Depression, Eygpt*. USGS Profe., Denver.

Breecker D. O., Sharp Z. D. and McFadden L. D. (2009) Seasonal bias in the formation and stable isotopic composition of pedogenic carbonate in modern soils from central New Mexico, USA. *Geol. Soc. Am. Bull.* **121**, 630–640.

Braun D. R., Levin N. E., Stynder D., Herries A. I. R., Archer W., Forrest F., Roberts D. L., Bishop L. C., Matthews T., Lehmann S. B., Pickering R. and Fitzsimmons K. E. (2013) Mid-Pleistocene Hominin occupation at Elandsfontein, Western Cape, South Africa. *Quat. Sci. Rev.* **82**, 145–166.

Clayton R. N., Friedman I., Graf D. L., Mayeda T. K., Meents W. F. and Shimp N. F. (1966) The origin of saline formation waters 1. Isotopic composition. *J. Geophys. Res.* **71**, 3869–3882.

Correa de Araujo J., Moreira E. L., Moraes V. C. A., Moreira A. P. D. and Soares G. D. A. (2011) A new possible atomic arrangement for the carbon atom in the B-sites of Ab-type carbonate apatite. *Mater. Res.* **14**, 376–379.

Cuffey K. M., Clow G. D., Alley R. B., Stuvier M., Waddington E. D. and Saltus R. W. (1995) Large arctic temperature change at the Wisconsin–Holocene glacial transition. *Science* **270**, 455–458.

DeNiro M. (1987) Stable isotopy and archaeology. *Am. Sci.* **75**, 182–191.

Dennis K. J., Affek H. P., Passey B. H., Schrag D. P. and Eiler J. M. (2011) Defining an absolute reference frame for "clumped" isotope studies of CO_2. *Geochim. Cosmochim. Acta* **75**, 7117–7131.

Dennis K. and Schrag D. (2010) Clumped isotope thermometry of carbonatites as an indicator of diagenetic alteration. *Geochim. Cosmochim. Acta* **74**, 4110–4122.

Diffendal R. F. (1995) Geology of the Ogallala/high plains regional aquifer system in Nebraska. In *Geologic Field Trips in Nebraska and Adjacent Parts of Kansas and South Dakota: Parts of the 29th Annual Meetings of the North-Central and South-Central Sections, Geological Society of America* (ed. C. A. Flowerday). Geological Society of America, pp. 61–75.

Duller R. A., Whittaker A. C., Swinehart J. B., Armitage J. J., Sinclair H. D., Bair A. and Allen P. A. (2012) Abrupt landscape change post-6 Ma on the central Great Plains, USA. *Geology* **40**, 871–874.

Eagle R. A., Eiler J. M., Tripati a. K., Ries J. B., Freitas P. S., Hiebenthal C., Taviani M., Elliot M., Marenssi S., Nakamura K., Ramirez P. and Roy K. (2013) The influence of temperature and seawater carbonate saturation state on ^{13}C–^{18}O bond ordering in bivalve mollusks. *Biogeosci. Dis.* **10**, 4591–4606.

Eagle R. A., Schauble E. A., Tripati A. K., Tütken T., Hulbert R. C. and Eiler J. M. (2010) Body temperatures of modern and extinct vertebrates from ^{13}C–^{18}O bond abundances in bioapatite. *Proc. Natl. Acad. Sci. U.S.A.* **107**, 10377–10382.

Eagle R. A., Tütken T., Martin T. S., Tripati A. K., Fricke H. C., Connely M., Cifelli R. L. and Eiler J. M. (2011) Dinosaur body temperatures determined from isotopic (^{13}C–^{18}O) ordering in fossil biominerals. *Science* **333**, 443–445.

Eberth D. a., Britt B. B., Scheetz R., Stadtman K. L. and Brinkman D. B. (2006) Dalton Wells: geology and significance of debris-flow-hosted dinosaur bonebeds in the Cedar Mountain Formation (Lower Cretaceous) of eastern Utah, USA. *Palaeogeogr. Palaeoclimatol. Palaeoecol.* **236**, 217–245.

Eiler J. (2007) "Clumped-isotope" geochemistry—the study of naturally-occurring, multiply-substituted isotopologues. *Earth Planet. Sci. Lett.* **262**, 309–327.

Eiler J. M. (2011) Paleoclimate reconstruction using carbonate clumped isotope thermometry. *Quat. Sci. Rev.* **30**, 3575–3588.

Eiler J. M. and Schauble E. (2004) $^{18}O^{13}C^{16}O$ in Earth's atmosphere. *Geochim. Cosmochim. Acta* **68**, 4767–4777.

Elliott J. C. (2002) Calcium phosphate biominerals. *Rev. Mineral. Geochem.* **48**, 427–453.

Fayek M., Harrison T., Grove M., McKeegan K. D., Coath C. D. and Boles J. R. (2001) In situ stable isotopic evidence for protracted and complex carbonate cementation in a petroleum reservoir, North Coles Levee, San Joaquin Basin, California, USA. *J. Sediment. Res.* **71**, 444–458.

Fricke H. and Wing S. (2004) Oxygen isotope and paleobotanical estimates of temperature and $\delta^{18}O$–latitude gradients over North America during the early Eocene. *Am. J. Sci.* **304**, 612–635.

Ghosh P., Adkins J., Affek H., Balta B., Guo W., Schauble E. A., Schrag D. and Eiler J. M. (2006) ^{13}C–^{18}O bonds in carbonate minerals: a new kind of paleothermometer. *Geochim. Cosmochim. Acta* **70**, 1439–1456.

Guo W., Mosenfelder J. L., Goddard W. A. and Eiler J. M. (2009) Isotopic fractionations associated with phosphoric acid digestion of carbonate minerals: insights from first-principles theoretical modeling and clumped isotope measurements. *Geochim. Cosmochim. Acta* **73**, 7203–7225.

Guthrie D. R. (1990) *Frozen fauna of the mammoth steppe: the story of Blue Babe*. The Univ. of Chicago Press, Chicago.

Guthrie M. L. (1988) *Blue Babe: the story of a steppe bison mummy from Ice Age Alaska*. White Mammoth, Fairbanks.

Harris C., Burgers C., Miller J. and Rawfoot F. (2010) O and H-isotope record of Cape Town rain fall from 1996 to 2008, and its application to recharge studies of Table Mountain groundwater, South Africa. *S. Afr. J. Geol.* **113**(1), 33–56.

Henkes G. A., Passey B. H., Wanamaker A. D., Grossman E. L., Ambrose W. G. and Carroll M. L. (2013) Carbonate clumped isotope compositions of modern marine mollusk and brachiopod shells. *Geochim. Cosmochim. Acta* **106**, 307–325.

Hintze L. F. (1993) *Geologic History of Utah*. Brigham Young University.

Huntington K. W., Eiler J. M., Affek H. P., Guo W., Bonifacie M., Yeung L. Y., Thiagarajan N., Passey B., Tripati A., Daëron M. and Came R. (2009) Methods and limitations of 'clumped' CO2 isotope (Δ_{47}) analysis by gas-source isotope ratio mass spectrometry. *J. Mass Spectrom.* **44**, 1318–1329.

IAEA (International Atomic Energy Agency). (2013) Global Network for Isotopes in Precipitation, (last accessed December, 2013): http://www.naweb.iaea.org/napc/ih/IHS_resources_gnip.html.

Jouzel J., Hoffmann G., Koster R. and Masson V. (2000) Water isotopes in precipitation: data/model comparison for present-day and past climates. *Quat. Sci. Rev.* **19**, 363–379.

Kaakinen A., Passey B. H., Zhang Z.Q., Liu L. P., Pesonen L. J. and Fortelius Mikael. (2013) Stratigraphy and paleoecology of the classical dragon bone localities of Baode County, Shanxi Province. In *Fossil Mammals of Asia: Neogene Biostratigraphy and Chronology* (eds. X. Wang, L. J. Flynn and M. Fortelius). pp. 29–90.

Kappelman J., Simons E. L. and Swisher C. C. I. (1992) New age determinations for the eocene–oligocene boundary sediments in the Fayum Depression, Northern Egypt. *J. Geol.* **100**, 647–667.

Kim S. and O'Neil J. (1997) Equilibrium and nonequilibrium oxygen isotope effects in synthetic carbonates. *Geochim. Cosmochim. Acta* **61**, 3461–3475.

Kirkland J. I. and Madsen S. K. (2007) The lower cretaceous cedar mountain formation, Eastern Utah: the view up an always interesting learning curve. In Field Guide to Geological excursions in southern Utah, (ed. Lund, W.R.) Geological Society of America Rocky Mountain Section. *Utah Geological Association Publication* **35**, 1–108.

Koch P. L., Tuross N. and Fogel M. L. (1997) The effects of sample treatment and diagenesis on the isotopic integrity of carbonate in biogenic hydroxylapatite. *J. Archaeol. Sci.* **24**, 417–429.

Kocsis L., Trueman C. N. and Palmer M. R. (2010) Protracted diagenetic alteration of REE contents in fossil bioapatites: direct evidence from Lu–Hf isotope systematics. *Geochim. Cosmochim. Acta* **74**, 6077–6092.

Kohn M. J. (1996) Predicting animal $\delta^{18}O$: accounting for diet and physiological adaptation. *Geochim. Cosmochim. Acta* **60**, 4811–4829.

Kohn M. and Cerling T. (2002) Stable isotope compositions of biological apatite. In *Phosphates: geochemical, geobiological, and materials importance* (eds. M. J. Kohn, J. Rakovan and J. M. Hughes), pp. 455–488. Reviews in Mineralogy and Geochemistry. Mineralogical Society of America, Washington, DC.

Kohn M. J. and Law J. M. (2006) Stable isotope chemistry of fossil bone as a new paleoclimate indicator. *Geochim. Cosmochim. Acta* **70**, 931–946.

Kohn M. J. and Zanazzi (2008) Carbon isotopes in fossil sequences as aridity proxies. *Geol. Soc. Am. Abstr. Programs* **40**, 169.

Kohn M., Schoeninger M. and Barker W. (1999) Altered states: effects of diagenesis on fossil tooth chemistry. *Geochim. Cosmochim. Acta* **63**, 2737–2747.

Kolodny Y., Luz B. and Navon O. (1983) Oxygen isotope variations in phosphate of biogenic apatites, I. Fish bone apatite—rechecking the rules of the game. *Earth Planet. Sci. Lett.* **64**, 398–404.

Laury R. (1980) Paleoenvironment of a late Quaternary mammoth-bearing sinkhole deposit, Hot Springs, South Dakota. *Geol. Soc. Am. Bull.* **91**, 465–475.

Lécuyer C., Balter V., Martineau F., Fourel F., Bernard A., Amiot R., Gardien V., Otero O., Legendre S., Panczer G., Simon L. and Martini R. (2010) Oxygen isotope fractionation between apatite-bound carbonate and water determined from controlled experiments with synthetic apatites precipitated at 10–37°C. *Geochim. Cosmochim. Acta* **74**, 2072–2081.

Lee-Thorp J. A. and Van der Merwe N. J. (1987) Carbon isotope analysis of fossil bone apatite. *S. Afr. J. Sci.* **83**, 712–715.

Levin N. E., Cerling T. E., Passey B. H., Harris J. M. and Ehleringer J. R. (2006) A stable isotope aridity index for terrestrial environments. *Proc. Natl. Acad. Sci. U.S.A.* **103**, 11201–11205.

Luyt J., Lee-Thorp J. A. and Avery G. (2000) New light on Middle Pleistocene west coast environments from Elandsfontein, Western Cape Province, South Africa. *South Afr. J. Sci.* **96**, 399–403.

Neuendorf, K. K. E., Mehl, J. P. and Jackson, J. A. (eds.) (2005) *Glossary of Geology*, 5th ed. Alexandria, VA.

NOAA (National Oceanographic and Atmospheric Administration). (2013) National Climatic Data Center, (Last Accessed December, 2013): http://www.ncdc.noaa.gov/.

Passey B. H., Cerling T. E., Perkins M. E., Voorhies M. R., Harris J. M. and Tucker S. T. (2002) Environmental change in the great plains: an isotopic record from fossil horses. *J. Geol.* **110**, 123–140.

Passey B. H. and Henkes G. A. (2012) Carbonate clumped isotope bond reordering and geospeedometry. *Earth Planet. Sci. Lett.* **351–352**, 223–236.

Passey B. H., Ayliffe L. K., Kaakinen A., Zhang Z., Eronen J. T., Zhu Y., Zhou L., Cerling T. E. and Fortelius M. (2009) Strengthened East Asian summer monsoons during a period of high-latitude warmth? Isotopic evidence from Mio-Pliocene fossil mammals and soil carbonates from northern China. *Earth Planet. Sci. Lett.* **277**, 443–452.

Passey B. H., Levin N. E., Cerling T. E., Brown F. H. and Eiler J. M. (2010) High-temperature environments of human evolution in East Africa based on bond ordering in paleosol carbonates. *Proc. Natl. Acad. Sci. U.S.A.* **107**, 11245–11249.

Pasteris J., Wopenka B. and Valsami-Jones E. (2008) Bone and tooth mineralization: why apatite? *Elements* **4**, 97–104.

Piga G., Santos-Cubedo A., Moya Solà S., Brunetti A., Malgosa A. and Enzo S. (2009) An X-ray Diffraction (XRD) and X-ray Fluorescence (XRF) investigation in human and animal fossil bones from Holocene to Middle Triassic. *J. Archaeol. Sci.* **36**, 1857–1868.

Quade J., Eiler J., Daëron M. and Achyuthan H. (2013) The clumped isotope geothermometer in soil and paleosol carbonate. *Geochim. Cosmochim. Acta* **105**, 92–107.

Rogers K. (1984) Herpetofaunas of the Big Springs and Hornet's Nest Quarries (Northeastern Nebraska, Pleistocene: Late Blancan). In *Transactions of the Nebraska Academy of Sciences and Affiliated Societies, Paper 240*. University of Nebraska Digital Commons, Lincoln, Nebraska, pp. 81–94.

Savin S. M. (1980) Oxygen and hydrogen isotope effects in low-temperature mineral–water interactions. In *The Terrestrial Environment: Handbook of Environmental Isotope Geochemistry* (eds. A. P. Fritz and J. C. Fontes). Elsevier, Amsterdam, pp. 283–327.

Schauble E. a., Ghosh P. and Eiler J. M. (2006) Preferential formation of ^{13}C–^{18}O bonds in carbonate minerals, estimated using first-principles lattice dynamics. *Geochim. Cosmochim. Acta* **70**, 2510–2529.

Schoeninger M. J. and DeNiro M. J. (1982) Carbon isotope ratios of apatite from fossil bone cannot be used to reconstruct diets of animals. *Nature* **297**, 577–578.

Seiffert E. R. (2006) Revised age estimates for the later Paleogene mammal faunas of Egypt and Oman. *Proc. Natl. Acad. Sci. U.S.A.* **103**, 5000–5005.

Snell K. E., Thrasher B. L., Eiler J. M., Koch P. L., Sloan L. C. and Tabor N. J. (2013) Hot summers in the Bighorn Basin during the early Paleogene. *Geology* **41**, 55–58.

Suarez M. B., Passey B. H. and Kaakinen a. (2011) Paleosol carbonate multiple isotopologue signature of active East Asian summer monsoons during the late Miocene and Pliocene. *Geology* **39**, 1151–1154.

Swinehart J. B., Souders V. L., DeGraw H. M. and Diffendal R. F. J. (1985) Middle Miocene to recent stratigraphy and paleogeography of western Nebraska. In *Proceedings of the Nebraska Academy of Sciences including GNATS & TER-QUA Divisions, and Nine Affiliates Societies, 95th Annual Meeting*. University of Nebraska Digital Commons, Lincoln, Nebraska, p. 56.

Thiagarajan N., Adkins J. and Eiler J. (2011) Carbonate clumped isotope thermometry of deep-sea corals and implications for vital effects. *Geochim. Cosmochim. Acta* **75**, 4416–4425.

Tripati A. K., Eagle R. A., Thiagarajan N., Gagnon A. C., Bauch H., Halloran P. R. and Eiler J. M. (2010) ^{13}C–^{18}O isotope signatures and "clumped isotope" thermometry in foraminifera and coccoliths. *Geochim. Cosmochim. Acta* **74**, 5697–5717.

Tierney J. E., Russel J. M., Huang Y., Sinninghe Damsté J. S., Hopmans E. C. and Cohen A. S. (2008) Northern Hemisphere controls on tropical southeast African climate during the past 60,000 years. *Science* **322**, 252–255.

Trueman C. N. and Tuross N. (2002) Trace elements in recent and fossil bone apatite. *Rev. Mineral. Geochemistry* **48**, 489–521.

Tuross N., Behrensmeyer A. K. and Eanes E. D. (1989) Strontium increases and crystallinity changes in taphonomic and archaeological bone. *J. Archaeol. Sci.* **16**, 661–672.

Tütken T. (2003) Die Bedeutung der Knochenfruhdiagenese fur die Erhaltungsfahigkeit in vivo erworbener Element- und Isotopenzusammensetzungen in fossilen Knochen. Thesis, Universitat Tubingen.

Tütken T., Vennemann T. W. and Pfretzschner H.-U. (2004) Analyse stabiler und radiogener Isotope in archaologishem Skelettmaterial: Herkunftsbestimmung des karolingishen Maultiers von Frankenthal und Vergleich mit spatpleistozanen GroBsaugerknochen aus den Rheinablagerungen. *Praehist. Zeitsch.* **79**, 89–110.

Tütken T., Vennemann T. W. and Pfretzschner H.-U. (2008) Early diagenesis of bone and tooth apatite in fluvial and marine settings: Constraints from combined oxygen isotope, nitrogen and REE analysis. *Palaeogeogr. Palaeoclimatol. Palaeoecol.* **266**, 254–268.

Tütken T., Vennemann T. W. and Pfretzschner H.-U. (2011) Nd and Sr isotope compositions in modern and fossil bones – proxies for vertebrate provenance and taphonomy. *Geochim. Cosmochim. Acta* **75**, 5951–5970.

Vachon R. W., Welker J. M., White J. W. C. and Vaughn B. H. (2010) Monthly precipitation isoscapes ($\delta^{18}O$) of the United States: Connections with surface temperatures, moisture source conditions, and air mass trajectories. *J. Geophys. Res.* **115**, D21126.

VanDeVelde J. H., Bowen G. J., Passey B. H. and Bowen B. B. (2013) Climatic and diagenetic signals in the stable isotope geochemistry of dolomitic paleosols spanning the Paleocene–Eocene boundary. *Geochim. Cosmochim. Acta* **109**, 254–267.

Wang Y., Xu Y., Khawaja S., Passey B. H., Zhang C., Wang X., Li Q., Tseng Z. J., Takeuchi G. T., Deng T. and Xie G. (2013) Diet and environment of a mid-Pliocene fauna from southwestern Himalaya: Paleo-elevation implications. *Earth Planet. Sci. Lett.* **376**, 43–53.

Wheeler E. J. and Lewis D. (1977) An X-ray study of the paracrystalline nature of bone apatite. *Calcif. Tiss. Res.* **24**, 243–248.

Zanazzi A., Kohn M. J., McFadden B. J. and Terry D. O. (2007) Large temperature drop across the Eocene–Oligocene central North America. *Nature* **445**, 639–642.

Zazzo A., Lecuyer C., Sheppard S. M. F., Grandijean P. and Mariotti A. (2004) Diagenesis and the reconstruction of paleoenvironments: A method to restore original $d^{18}O$ values of carbonate and phosphate from fossil tooth enamel. *Geochim. Cosmochim. Acta* **68**, 2245–2258.

Zhu Y., Zhou L., Mo D., Kaakinen A., Zhang Z. and Fortelius M. (2008) A new magnetostratigraphic framework for late Neogene Hipparion Red Clay in the eastern Loess Plateau of China. *Palaeogeogr. Palaeoclimatol. Palaeoecol.* **268**, 47–57.

Associate editor: Edwin Schauble